# Chapter 10

# 3-D Modelling of Biological Systems for Biomimetics

*Shujun Zhang*,*,† *Donghui Chen*,† *Kevin Hapeshi** *and Xu Zhang*‡

**School of Computing and Technology, University of Gloucestershire, UK*

*†Key Laboratory of Bionics Engineering, Ministry of Education, Jilin University, China*

*‡CED Group of Rolls-Royce UTC, Faculty of Engineering and the Environment, University of Southampton, UK*

With the advanced development of computer-based enabling technologies, many engineering, medical, biology, chemistry, physics and food science etc have developed to the unprecedented levels, which lead to many research and development interests in various multi-discipline areas. Among them, biomimetics is one of the most promising and attractive branches of study. Biomimetics is a branch of study that uses biological systems as a model to develop synthetic systems. To learn from nature, one of the fundamental issues is to understand the natural systems such animals, insects, plants and human beings etc. The geometrical characterisation and representation of natural systems is an important fundamental work for biomimetics research. 3D modeling plays a key role in the geometrical characterisation and representation, especially in computer graphical visualization. This chapter firstly presents the typical procedure of 3D modelling methods

and then reviews the previous work of 3D geometrical modelling techniques and systems developed for industrial, medical and animation applications. Especially the chapter discusses the problems associated with the existing techniques and systems when they are applied to 3D modelling of biological systems. In addition, the chapter also presents two case studies of authors' own work. Based upon the discussions, the chapter proposes some areas of research interests in 3D modelling of biological systems and for Biomimetics.

## 10.1. Introduction

Biomimetics is a branch of study that uses natural biological systems as a model to develop synthetic systems. While approaches vary, the principle is the same in that using biomimetics, human beings learn from nature. Biomimetics is also known by several names — bionics and biognosis, etc. Basically it is the concept of taking ideas from nature and implementing them in another technology such as engineering, design and computing. The concept is very old (the Chinese wanted to make artificial silk 3,000 years ago; in Greek mythology Daedalus' wings could be regarded as an early design failure). Biomimetics is gathering momentum because of recent advances in technology and the ever increasing need for sympathetic and sustainable technology. For details of the definition and discussion of biomimetics, please refer to Refs. 1–3.

To learn from nature, one of the fundamental issues is to understand the biological systems. The understanding consists of (1) the description of the natural system as well as its behaviors and functions; (2) the specification of the mechanisms of how natural systems perform their functions; (3) the identification of the physical, chemical and biological properties of natural systems; (4) the geometrical characterization of natural systems including morphological surface features and internal structures and (5) any other related areas which are useful for the design and development of synthetic systems. Among the above areas, the geometrical characterization of natural systems is the important fundamental work for biomimetics research. Since human beings looked to nature for inspiration more than 3,000 years when the

Chinese hankered after an artificial silk,[2] people have been using various methods to obtain the geometrical information of natural systems. Many people have published their work on geometrical characterization of animals, insects, plants and human beings.[4–39] The work includes techniques for acquisition of geometrical information, data processing algorithms, 3-D modelling algorithms, 3-D geometrical computation theory and methods for computer graphical visualizations. However, most of these technologies and methods have been designed and developed for engineering, medical-related application and animation purposes. When they are applied to 3-D modelling of biological systems for biomimetics research and applications, many problems often emerge. These problems include: (1) unsuitable accuracy, resolution and workable areas of 3-D scanners for raw data capturing of biological objects; (2) low efficiency algorithms for raw data pre-processing, point cloud/image edge detection and segmentation; (3) 3-D geometrical mathematical models for 3-D modelling, representation and computer graphical visualization of biological objects with special features such as sharp corners of a biological object, insect tarsus, field mouse hairs and tine features of flowers of some plants, etc.; (4) as far as the authors are aware, there is no dedicated 3-D modelling system for biological objects, including scanners, associated software and stand-alone software; and (5) there is no well-accepted methodology/protocol in the biomimetics community for people to follow in enhancing quick information sharing, efficient knowledge generation and promotion. This chapter tries to discuss those problems, present some typical applications and propose some areas of research interests with the purpose of presenting problems, and hopefully attracting more people's interests in efforts for design and development of systems suitable for 3-D modelling of biological objects.

To avoid the repetition, in this chapter, for convenience, the term "biological objects" will be used to refer to all complex biological systems, namely animals, insects, plants and human beings. The size of a biological object can be as big as a mammal animal,or as small as an insect and as tiny as a cell.

Following the introduction, Section 10.2 will present the discussion of the methods for 3-D geometrical modelling used in practice. The discussion will be focused on the methods for raw

data capturing, pre-processing, edge detection and segmentation, including the problems of the existing 3-D modelling technology and methods, especially the problems when they are applied to 3-D modelling of biological objects. Section 10.3 will present the typical 3-D digitizing technologies/scanners, their characteristics and suitability for digitizing biological objects. Section 10.4 will discuss various 3-D geometrical mathematical modelling methods and their characteristics. Then, Section 10.5 will present three applications of 3-D modelling to biomimetics study. Based upon the above sections, Section 10.6 will propose some areas of interest for 3-D modelling of biological objects, and finally Section 10.7 tries to draw conclusions.

## 10.2. 3-D Geometrical Modelling

### 10.2.1. *Introduction*

3-D geometrical models of a physical object can be defined as a data set in an organized numerical form. They can be used to generate various 3-D models of different formats to graphically represent the object. Computer graphical visualization is the most popular and powerful method. There are many 3-D computer models used in engineering, science, medical, military, arts and many other areas. The list can grow much longer easily. The methods for generation of the 3-D computer models can be classified into two main types: one is reverse engineering (RE), which is currently used widely for industrial and animation applications. RE is the process of duplicating an existing component or subassembly without the aid of drawings, documentation or computer model data by using 3-D geometry computation, computer graphics, engineering analysis and measurement of existing parts to develop technical data required for successful commercial reproduction.[40,41] In this chapter, the RE-based method is called **Method 1 (M1)**; the other method is direct generation on computer through 3-D computer software such as Solid Works and Auto CAD etc., called **Method 2 (M2)**. The difference between the two methods is that the RE method employs 3-D digitizing techniques to obtain the surface information of a physical object in the form of a set of geometrical points of three position components,[42] and sometimes three surface color information,[43] while the direct generation of a

3-D model is mainly based on the human–computer interface of 3-D software to input the geometrical information. That is, almost all geometrical information is obtained using 3-D digitizing scanners in the RE method while the direct 3-D generation method employs limited geometrical information mainly from manual measurement of an existing object. Figure 10.1 shows the 3-D models of engineering components, animals, insects, and plants generated using M2.[44,45] These models are certainly useful for biomimetics study. However, they lack detailed geometrical information about the morphological surfaces; so many small but very important surface features have been ignored. Comparatively, there are more problems associated with M1; this is especially true when the method is applied in 3-D modelling of a biological object. Besides, M2 can be seen loosely as a sub-set of M1. So this section will mainly present M1 procedures and discuss the associated problems.

## 10.2.2. *Procedure of M1*

### 10.2.2.1. *Procedure*

The procedure of typical M1 consists of five steps for CAD model creation. It involves data acquisition, data processing, segmentation, curve and surface model generation and solid model creation, as shown in Fig. 10.2.

**Fig. 10.1.** 3-D models of engineering component, animals and plants generated using Method 1. Some jpg files of this figure were from 3D Café and 3D Model Works (www.3dcafestore.com/3dmodels1.html, http://3dlenta.com/en/plants.html).

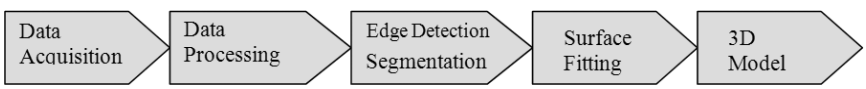


**Fig. 10.2.** The five steps of a typical M1.

#### 10.2.2.2. *Data acquisition*

Data acquisition is the first step in M1. A target component (e.g. a morphological surface of an animal, insect or plant) is normally scanned using an appropriate scanning strategy and 3-D digitizing equipment. Several settings may be required for a full scanning of a complex surface. At each scanning, the geometrical positions of many points on the surface and surface color information are captured. The position of each geometrical point is described by three positional co-ordinate components, $x$, $y$, and $z$. The color of the surface is described by three color components, r (red), g (green) and b (blue). All points together are called the point cloud.

The surface information of an object can also be captured by normal video or CCD cameras used for Photogrammetry, a technology which has been used for more than 150 years,[46–50] or for Photogeometry, a process in which a series of still photos of an object are taken and a combination of proprietary and off-the-shelf software is used to derive a 3-D representation of an object in space.

The above scanning methods can only be used to acquire the geometrical and color information of the surface of an object without slicing it. No information of internal features can be obtained. So various other technologies have been developed to address this problem. The typical methods are to obtain the cross section information by either directly scanning or cutting the object into a serial of cross sections[51] for medical-related applications. Medical imaging has come a long way since 1895, when German physicist Wilhelm Conrad Röntgen observed strange flickers cast by his cathode-ray instruments. Within months, Röntgen had used the mysterious "X-rays," as he called them, to produce an image of the bones of his wife's hand, revolutionizing medicine. For the first time, physicians could peek inside the body without cutting it open or probing an orifice.

3-D scanners for medical-related applications are normally serial cross-section based. Capturing technologies include (1) sections obtained directly (e.g. serial-section microscopy, confocal microscopy, or mechanical sectioning of an object); (2) serial sections obtained from MRI (magnetic resonance imaging), CT (computer tomographic reconstruction), ultrasound and X-ray; (3) 3-D holography; and

(4) direct calculation from mathematical models, etc. In this chapter, we refer these methods as serial cross-section based 3-D scanning methods.

In engineering applications, some efforts have been made to build 3-D models of porous materials using microscope to capture the images of sliced surfaces of the porous materials and then processing these images using various software and algorithms.[52] The advantage of this method is that the accuracy of the model can be as high as a few microns though the proper selection of the magnifying factor of the microscope. However, this is a very time-consuming process. For example, to build a 3-D model of 2 mm by 9 mm by 9 mm porous metal could take up to two to three months.

#### 10.2.2.3. *Data processing*

Data processing mainly consists of two tasks: (1) point clouds alignment to form a single point cloud to represent the whole surface and (2) point cloud sampling.

### (a) Point clouds alignment

As discussed above, it is very often required to have several settings to obtain a full scanning of a surface, so more than one point clouds are collected. They should be assigned together to form a single point cloud. There are normally two ways to do it: (1) Physical method — alignment through a single physical scanning reference point or multi physical scanning reference points and a homogenous matrix describing the positional and orientation relationships between the reference points; (2) Soft computing method — alignment by picking several (at least three) non-collinear points (at least one point should not be co-planar to the other two) of each cloud to generate a homogenous matrix. The physical method is easy to use, but it takes long time and it is more expensive to make additional fixtures for setting up the object. The errors of this method are dependent on both the quality of the fixtures and the experience of the operators. The soft computing method is relative cheap and easy to use. but it demands good mathematical models for the efficient computation of the homogeneous matrices. Some scanners and associated software provide this feature. But it is often found that the performance of

this feature is not as good as claimed by the marketing promotion activities.[41,53]

## (b) Sampling methods

Before or after alignment of the point clouds, due to the nature of three-dimensional scanners, the number of scanned points is often large, and accuracy varies. The number can be from millions to billions. A large number of data points cannot be manipulated efficiently in late processing and application. So, it is desirable to appropriately reduce the number of data points. However, it needs to be determined precisely how many (or at what interval) points will be sampled. This amounts to saying that original parts cannot be reconstructed correctly if the scanned data is sampled beyond the tolerance.

In this chapter, the two sampling methods will be discussed: vector sampling and rate sampling.[54,55]

The algorithm for the vector sampling method can be described as follows:

Suppose there are three consecutive scanned points ($\boldsymbol{P}_a$,$\boldsymbol{P}_b$,$\boldsymbol{P}_c$) from a point set. Then, two directional vectors can be computed with the points: $\underline{\boldsymbol{V}}_1 = \boldsymbol{P}_b - \boldsymbol{P}_a$ and $\underline{\boldsymbol{V}}_2 = \boldsymbol{P}_c - \boldsymbol{P}_b$. The idea of the vector sampling method is to remove the center point ($\boldsymbol{P}_b$) if the angle ($\theta$) between two direction vectors, $\underline{\boldsymbol{V}}_1$ and $\underline{\boldsymbol{V}}_2$, is less than the predefined angle tolerance ($\theta_t$). At the same time, the distance between first two points ($\boldsymbol{P}_a$ and $\boldsymbol{P}_b$) must be taken into account. If the distance ($l = |\boldsymbol{P}_a - \boldsymbol{P}_b|$) from a considered point to the last retained point is larger than the distance tolerance ($l_t$), the considered point will be preserved.

Sampling by rate is a simple but powerful technique to reduce highly redundant points within a given tolerance. This method removes every point whose sequence number is a multiple of "$\alpha$" along a scan line, where $\alpha$ is the value of a user-input integer. Both methods are often employed together for sampling point clouds.

For images stack captured using serial cross-section based 3-D scanning methods, some pre-processing work is required for image enhancement prior to 3-D reconstruction. The pre-processing usually involves application of **image filters** (*mathematical algorithms*

*implemented in software*) to the entire data set to remove noise and artifacts, smooth or sharpen the images, or to correct for problems with contrast and/or brightness. While these filters are generally performed as pre-processing steps, they can also be carried out after a 3-D model has been reconstructed from the image stack.

Median and Gaussian filters have the general effect of smoothing images. These are used to eliminate noise and background artifacts and to smooth sharp edges, but also tend to remove some of the details in small objects. This kind of filter is useful if we want a smooth 3-D surface model of biological objects.

Sharpening filters can be used to emphasize details in the image stack, but also have the effect of highlighting noise and other small artifacts. The application of sharpening filters is most useful when the image stack consists of fine structural components of a specimen, or when edge enhancement is desired. This kind of filter is useful if we want a 3-D model with small features of biological objects. However, this function sometimes cannot be applied when modelling a biological object for the applications of design and development of a tool that needs a sharper edge.

The contrast and brightness of the image stack can be adjusted to enhance perception of the sampled specimen. This is usually done by changing the ramping of the greyscale values for the dataset. Histogram equalization can be used to improve contrast by a non-linear mapping of the grey levels in an image. This technique is most commonly used when the grey levels are concentrated in a small portion of the range of possible values.

It is important to realize that the application of filters to the data set can ultimately affect quantitative measurements of 3-D reconstructions produced from it. As such, the application of filters in some instances is used only for display purposes.

#### 10.2.2.4. *Segmentation and edge detection*

#### (a) Edge detection

Edge points are either the outer boundary among constituent regions with relatively distinct discontinuities, or internal boundaries in a

region. Edge detection is a crucial step since geometrical features are recognized and extracted from the information of edge points.

There are normally two kinds of edge points: sharp edges and smooth edges. Sharp edge features can be often found on the surfaces of animals and plants. Sharp edges can be detected by the existence of tangency discontinuities. The process of sharp edge detection is straightforward since the existence of tangency discontinuities can be easily checked along the scan lines. But there are some errors here, since the points on the true edge could be omitted during the scanning. This error is dependent on the resolution of the scanner. This is often found to be a barrier to generating a satisfactory 3-D model of a biological object.

The variation of curvature values can be used to detect smooth edges. One characteristic provides a reasonable solution for detecting smooth edges in a curvature plot: "spike." These spikes in the curvature plot give a clear indication of the location at which the points are to be partitioned into different sets. Hence, the presence of spikes can then be used to detect the presence of smooth edges.

## (b) Segmentation

An ordinary engineering component or a biological object consists of many distinct geometric shapes. The whole scanned point cloud sometimes needs to be divided into several regions according to its constituent shapes. This process is called segmentation. The whole segmentation process needs to be successfully accomplished, since it is normally a prerequisite step to recognizing features from the discrete scanned data. It has been manually carried out by RE operators. The mouse is normally used to select appropriate points on the displayed image. The point data captured in the mouse "window" are ready to be mapped to a feature. Segmentation must be continued until the whole regions of an object are isolated completely. The level of subdivision depends upon the complexity of the object.

It is the trend that more work has been done for automatic segmentation though it is still in the early stage for the practical applications of fully automatic segmentation.[56] It is especially true for the method based RE with normal industrial 3-D digitizing scanners.

As for image stack obtained using serial cross-section based 3-D scanning methods, segmentation refers to the process of extracting the desired object (or objects) of interest from the background in an image or data volume. There are a variety of techniques that are used to do this,[57–59] ranging from the simple (such as thresh holding and masking) to the complex (such as edge/boundary detection, region growing and clustering algorithms). Segmentation can be aided through manual intervention or handled automatically through software algorithms. It can be performed before building the 3-D reconstruction by processing of images in the image stack, or after the 3-D model has been formed.

#### 10.2.2.5. *Curve/surface model creation*

The point clouds generated from segmentation can be used to generate curve/surface models using commercial software such as Imageware's Surfacer[60] and Raindrop Geomagic Studio,[61] etc. Various curve and surface models created at this stage are useful for biomimetics research and application for analyzing and understanding the functions and geometrical features of biological systems.

#### 10.2.2.6. *Solid model creation*

Solid models can be directly created from curve or surface models generated in Section 10.2.2.5 by using commercial CAD software such as Solid Edge or Solid Works, etc. Solid models are useful for simulation, animation performance analysis of biological systems, man-made system design and manufacturing in biomimetics research and application.

After pre-processing of the image stack captured using serial cross-section based 3-D scanning methods, it can then be reconstructed into a 3-D volumetric dataset. This is usually achieved using either volume or surface rendering techniques.

The resulting 3-D image from cross-section based methods such as NMR and confocal microscopy is normally a discrete scalar field, that is, it is a 3-D grid with values given at each point of the grid. But this kind of 3-D image is not very useful for biomimetics study.

**Volume rendering** is a computer graphics technique whereby the object or phenomenon of interest is sampled or subdivided into many

cubic building blocks, called ***voxels*** (or volume elements/pexel). A voxel is the 3-D counterpart of the 2-D pixel and is a measure of unit volume. Each voxel carries one or more values for some measured or calculated property of the volume and is typically represented by a unit cube. The 3-D voxel sets are assembled from multiple 2-D images and are displayed by projecting these images into 2-D pixel space where they are stored in a frame buffer.

In **surface rendering**, the volumetric data must first be converted into geometric primitives by a process such as isosurfacing, isocontouring, surface extraction or border following. These primitives (such as polygon meshes or contours) are then rendered for display using conventional geometric rendering techniques.

Both techniques have advantages and pitfalls. A major advantage of the volume rendering technique is that the 3-D volume can be displayed without any knowledge of the geometry of the dataset and hence without intermediate conversion to a surface representation. This conversion step in surface rendering can sometimes be quite complex, especially if surfaces are not well defined (i.e. noisy 2-D images) and can require a lot of user intervention (such as manual contour tracing). On the other hand, because the 3-D dataset is reduced to a set of geometric primitives in surface rendering, this can result in a significant reduction in the amount of data to be stored, and can provide fast display and manipulation of the 3-D reconstructions produced by this method. By contrast, since all of the image stack data is used for volume rendering, computers with lots of memory and processing power are required to handle volumes rendered in this manner. Because the entire dataset is preserved in volume rendering, any part, including internal structures and details (which may be lost when reducing to geometric structures with surface rendering) may be viewed. This could prove to be a powerful method for animation of biological systems to understand their principles and mechanisms at the early stage of biomimetics research.

## 10.3. 3-D Digitizing Technologies/Scanners

As discussed above, the first step of creating 3-D models of an existing physical object is to collect geometrical, and sometimes color,

information of the morphological surface and internal features of an object. In this step, 3-D digitizing technologies/scanners play the central role. There are a variety of commercially available technologies/scanners that can be used to digitize objects from the molecular scale on up to multi-story buildings. Many of the commercial products are available on the market. Based on the applications, 3-D scanners can generally be classified into three main categories: 3-D scanners for industrial applications, for medical applications and for animation applications.

### 10.3.1. *3-D scanners for industrial applications*

The main technologies used in 3-D scanners are sensing technologies including tracking, imaging, range finding or a combination of these. Based on the sensing technologies, 3-D scanners for industrial applications can be further divided into two sub-categories: contact and non-contact scanners.

#### 10.3.1.1. *Contact 3-D scanners*

The sensing technology in contact 3-D scanners is tracking systems that digitize by positioning a probe on the surface of an object and triggering the computer to record the location, as shown in Fig. 10.3. The simplest tracker is a mechanical linkage or pantograph. Computerized Measuring Machines (CMM), such as Cyclone made by Renishaw[42] and X330 by Faro Technologies[62] are robust 3-D mechanical trackers for manufacturing applications and landscape documentation and survey. There are manual and automated contact-tracking systems. Manual tracking systems requiring a large amount of patient, skilled labor like Faro Arm, but they can sometimes digitize an object directly into polygonal models, eliminating the need for the reconstruction phase. Automated probe tracking systems produce point clouds that will require fully reconstruction line Renishaw Cyclone. Most contact 3-D scanners are designed for the accuracy from 10 $\mu$m to 200 $\mu$m, which is suitable for industrial applications such as reverse engineering of an existing component and error analysis.[41,53] But some automated trackers such as the Scanning Probe Microscope (SPM) can be used to create 3-D models of molecular scale objects.

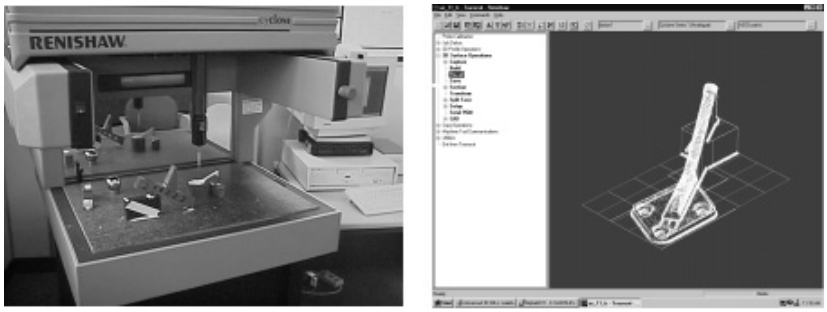


**Fig. 10.3.** (a) Part being scanned. (b) Point cloud collected by Cyclone 3D scanner.

**Fig. 10.4.** A contact 3-D scanner was used to find out the leg and body layout design of various insects.

3-D contact scanners can be used for biomimetics research in areas that do not need detailed geometrical features such as scanning the overall shape of a dolphin for CFD analysis to learn about its wonderful fluid dynamics performance[63–64] or to find out the leg and body layout design of various insects to study their incredible ability to carry loads or study their walking efficiency to advance man-made limbed machine innovation,[65–67] as shown in Fig. 10.4.

But most 3-D scanners for industrial applications are not suitable for biomimetics research that requires understanding and capturing small geometrical features of a biological object. For example, to learn from the female dung beetle's unique surface features to design and develop

low resistance and efficient earth-moving equipment such as bulldozers and ploughs,[4,7] it is necessary to scan its forehead, which requires scanners with much higher accuracy and resolution than normal 3-D contact scanners for industrial applications.

It is worth pointing out that a Japanese company, Mitutoyo, marketed a contact 3-D scanner which can capture geometrical information with the accuracy as high as $\pm$ (0.5 + L/100) $\mu$m, resolution as high as 0.1 $\mu$m and measuring force as small as 0.01 N,[68] that is suitable for scanning small geometrical features. But the scanner's range is only 50 mm and there is no confirmed report that size of the probe is small enough to reach the small features or that there is associated software that is suitable for biomimetics research.

#### 10.3.1.2. *Non-contact 3-D scanners*

The sensing technology in non-contact 3-D scanners involves tracking systems that digitize by emitting light (laser or normal) onto the object to capture the geometrical information in the form of three positional components (x, y, z) or three positional components (x, y, z) and three color components (r, g, b). The typical examples of this kind of 3-D scanner are Hymarc's Hyscan and Wicks Wilson's human body and head scanners.

The Hyscan 45 is a high-performance 3-D scanning laser digitizer which rapidly acquires precise XYZ data points from an object. Hyscan systems map surface information in a continuous high-speed non-contact fashion with $\pm 0.001''$ ($\pm 0.025$ mm) $\pm 3$ sigma accuracy, which satisfies demanding applications such as reverse engineering, design, rapid prototyping and inspection in industry. The Hyscan laser digitizer is designed to fit to any Coordinate Measuring Machine (CMM), Computer Numerically Controlled (CNC) Machine, or other translation device. The integrated design yields a powerful yet user friendly system which can be quickly and easily be interchanged with existing probes or tools.

Figure 10.5 shows the principle behind a 3-D laser scanner.[69–71] The TriForm Head Scanner from Wicks and Wilson is designed specifically to capture the human head in monochrome or full color. The capture technology is that the scanner projects striped patterns of

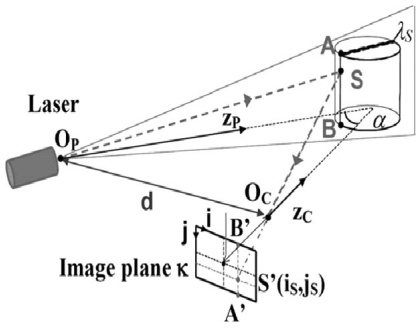


**Fig. 10.5.** Schematic diagram of laser scanning system.[69].

normal white light onto the subject, using no lasers or other radiation. The patterns are stored by a digital camera and image software is used to process 3-D geometrical and color information to create a full color 3-D image of head, including complex capturing of hair. The main advantage for this scanner is the light source is not lasers or other radiation that could damage the living object. The other advantages include very short scanning time (from about two seconds for HS1 SINGLE-VIEW to about 10 seconds for HS2 Double View) and color information of the surface is captured simultaneously. These features make this scanner suitable for scanning biological bodies (animals, insects and plants) for some biomimetics research that does not need high accuracy and resolution, since the TriForm scanners' accuracy is as low as $\pm 1$ mm.[43] Figure 10.6 shows the TriForm HS2 Double View Head Scanner.

There are many other 3-D scanners available on the market. For more scanner products and their working principles, please see Refs. 70 and 72. Most of them are not suitable for biomimetics research that requires the capture of small geometrical features of biological bodies.[8,67]

### 10.3.2. *3-D scanners for medical applications*

This section briefly discusses 3-D scanners mainly for medical-related applications from the biomimetics point of view. For more details, see Refs. 73 and 74. 3-D scanners for medical applications mainly rely

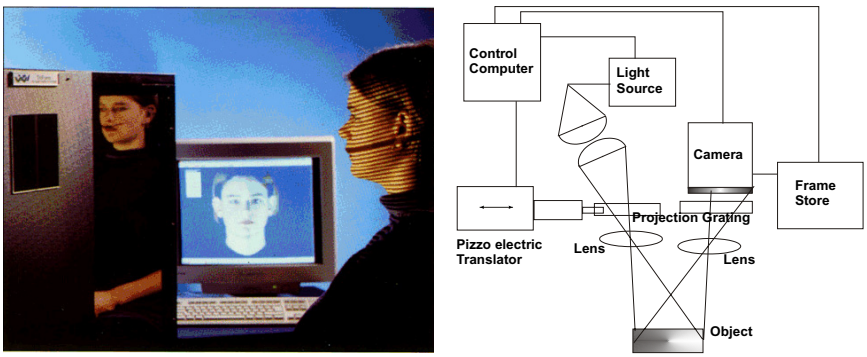


(a) (b)

**Fig. 10.6.** HS2 Double View Head Scanner and diagram of Auto-MATE System.[41]

on an image approach using a series of slices through the object. The slice image can be obtained by actually cutting the object and taking optical photographs of the ends or by using advanced sensors such as ultrasound, Magnetic Resonance Imaging (MRI), X-Ray Computed Tomography (CT), serial-section microscopy and confocal microscopy. The slices can be used to produce volumetric data (voxels) or feature extraction might be used on the images to produce contour lines. Both forms of data can be readily converted to polygonal and surface models.

In serial-section microscopy, the tissue being studied is sectioned into a number of slices and each slice is put into a microscope. Then, images are captured of each slice. To recreate how the tissue looked before we sectioned it, we must put all the images of all these slices back together again, just as if we were putting the real slices of tissue back together again.

In confocal microscopy, the microscope can obtain a single plane of image data without having to slice the tissue. In this case, we don't need to realign the images of the slices much, but just stack them back together and then visualize the result.

In MRI, the imaging device acquires a number of cross-sectional planes of data through the tissue being studied. All of these planes must be stacked back together to obtain a complete picture of what the tissue was like.

Problems associated with image acquisition using serial-cross-section-based 3-D scanners are discussed as follows:

(1) It is usually very expensive and requires a tightly controlled operational environment.
(2) The file size of the image stack is very large. For example, when using confocal microscopy, an image stack consisting of 50, 512*512 8-bit images occupies 12.8 MB of storage space. The 3-D size of the image stack not only has implications for storage space, but also has adverse effects on the processing, display and manipulation of this data. That could be a serious problem for 3-D modelling of biological objects.
(3) It is difficult to select thickness of the slice. If the thickness is too small, the number of slices is too high, which leads to large file size; if thickness is too big, some small features (like the boundary location between two distinct features) would be omitted.
(4) Confocal microscopy is highly destructive. As the laser scans the specimen, it is selectively bleached in the X/Y plane and non-selectively bleached in the Z plane. If the specimen is scanned one plane at a time, not only is that plane bleached, but all other cross-sectional planes above and below that plane are also bleached. If the laser power is set to its maximum, the bottom slice in an image stack would have received as much irradiation as if all of the images were captured at the same plane. It has been suggested that this non-selective bleaching effect in the Z plane can be reduced by a process called Z-axis distributed averaging.[75]
(5) It is usually more difficult to use serial-section microscopy and put the slices back together than to use confocal microscopy, MRI, or CT. However, it is more difficult to use an imaging technique like MRI or confocal microscopy to "see" a small object than to use serial-section microscopy. Because the information from surrounding areas blurs out what you're looking for, the smallest thing that an MRI can "see" is about 1mm cubed. For confocal microscopes, the smallest object that is detectable is about 1/10 $\mu$m (1/10,000 mm). But once you slice the object up, you can use other forms of microscopy such as an electron microscope to be able to see objects almost as small as

1/, $\mu$m (1/100,000,000 mm). There are even newer "atomic force" microscopes that even let you detect individual atoms, but not many people (as yet) have done 3-D reconstructions at this minute level. The problem is, the smaller one goes, the more artifacts can be introduced, so the reconstruction process gets much more difficult.

From the above discussion, it can be noted that serial cross-section based 3-D scanners can be a good choice for some biomimetics research such as understanding of a biological system's mechanisms at the early stage of biomimetics research. However, we are far from the situation where we can rely on them to meet all the requirements of biomimetics research and application.

### 10.3.3. *3-D scanners for animation applications*

Animation applications include art, fashion, clothing, film, e-Business, engineering system concept design, medical treatment such as prosthetics, orthopedic fittings, biopsy, radiation therapy, and robotic hip replacement, etc.

3-D scanners for animation applications are different from the others in terms of their relatively low cost and high efficiency of data acquisition. But the accuracy is not as high as that for industrial and medical applications. The typical accuracy is from 200 $\mu$m to 2 mm. There are also two kinds of scanners: contact and non-contact.

For example, the MicroScribe® G2[76] is an affordable 3-D digitizing system marketed more towards the animation industry. MicroScribe products capture the physical properties of three-dimensional objects and translate them into complete 3-D models. Wicks Wilson's normal white light scanners are also ideal for animation applications. Other scanners include the EOS Systems PhotoModeler, which uses manual feature digitizing in disparate viewpoint images to create object models. Geometrix introduced a product at Siggraph 1998 that applies automated photogrammetry to video images. This technology holds significant promise for rapid creation of 3-D models using conventional and digital video cameras. Figure 10.7 shows a Photogrammetry system and its principle.[77]

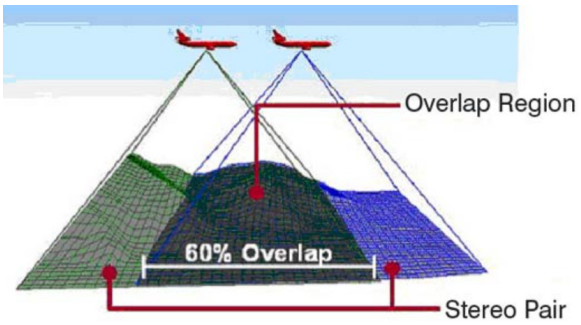


**Fig. 10.7.** Principle of Photogrammetry.[77]

Due to the nature of function performances such as low cost and high efficiency of data acquisition, 3-D scanners for animation applications can be used in biomimetics study that requires geometrical models of large size and low accuracy.

## 10.4. 3-D Geometrical Mathematical Modelling Methods

As for the 3-D modelling of cars, airplanes and engineering equipment, etc., Computer Aided Geometric Design (CAGD) plays a major role in 3-D modelling of animals, insects and plants for biomimetics research and development. The mathematics behind CAGD is also indispensable in computer graphical visualization of the models. There are many methods such as polynomial and parametric interpolation, least squares and Bezier curves, Hermite and natural cubic splines, tensor product surfaces, lofting and Coons surfaces, B-splines, B-spline curves and surfaces, interpolation with B-spline curves, least squares B-spline methods, and NURBS (non-uniform rational B-splines). This section discusses some mathematical modelling methods and their suitability for 3-D modelling of biological objects.

### 10.4.1. *Polynomial interpolation for curves*

The central idea of interpolation is to find a polynomial which goes through prescribed data points $(x_i, y_i, z_i)$, $0 \leq i \leq n$. Some methods

(such as Newton interpolation) can be used to find the unique $z = f(x, y)$ of degree less than or equal to $n$ — one less than the number of points. The mathematics for finding this equation is elementary and well known.[78–80] The main problems associated with polynomial interpolation for curve models are: (1) It cannot be trusted for extrapolation purposes, which indicates that it is not reliable for analysis and design of a product using geometrical information generated by extrapolation of the curve model obtained by scanning small area of biological objects for biomimetics research; (2) It inevitably generates wiggling of high degree polynomials within the range of interest. The wiggling problem can be solved using mathematical treatment.[80]

### 10.4.2. *Bezier curves*

Polynomial interpolation is suitable for a "best fit" polynomial of lower degree. If the number of points, $N$, is limited and a higher degree of polynomial is required, it is normally difficult to get an exact fit. The method of least squares is one popular solution for such circumstances. However, Bezier curve is another alternative. It starts with points $P_0, P_1, \ldots, P_n$ and ends up with a parametric curve that is polynomial of degree less than or equal to $n$ in each slot.

The Bezier curve associated with control points $P_0, P_1, \ldots, P_n$ is defined for $0 \leq t \leq 1$ by

$$B(t) = \sum_{i=0}^{n} \binom{n}{i} t^i (1-t)^{n-i} P_i. \tag{10.1}$$

The functions attached to the points here are known as the Bernstein basis functions. Cubic Bezier curves use four control points, and the basis functions are $(1-t)^3$, $3(1-t)^2$, $3(1-t)t^2$, $t^3$. These curves have many applications, sometimes in the equivalent Hermite formation, specified in terms of just two control points with specified tangent vectors there.[79] Large curves can be built up by stringing many such segments together, with tangent continuity at all points. This property can sometimes be found to be very useful in biomimetics. For example, due to limitation of workable range of 3-D scanners, a large area of biological surface can be divided into a matrix of small regular areas.

Then each small area can be scanned separately. The point cloud for each scanning can be directly processed using software to generate the desired Bezier curves based on the requirement of biomimetics research and application. All Bezier curves generated for each small area can be stringed together to form Bezier curves over the whole area. This method will save the multi-point clouds alignment time and reduce errors due to this alignment.

Bezier curves always lie within the convex hull of their control points, since on [0; 1] the Bernstein basis functions are clearly non-negative and sum to 1. Generally speaking, only the first and last control points are interpolated. The intermediate control points influence the curve's shape in a different way, acting more like magnets. This feature shows that Bezier curves cannot be used for the case that requires high accuracy in biomimetics research. There are various ways to adjust the influence of the control points. One could repeat some points, i.e., list them more than once, but increasing the number of points also increases the degree of the resulting curve. Another restriction inherent to the Bezier approach is the fact that the curves change totally as soon as one control point is moved. This makes it difficult to build 3-D models that require modifications at small local areas.

It can be noted that both polynomial interpolation and Bezier curve methods are limited to polynomials. Now let us not restrict to polynomials. Given points $\boldsymbol{P}_1, \boldsymbol{P}_2, \ldots, \boldsymbol{P}_n$ and corresponding "weights" $w_0, w_1, \ldots, w_n$, the associated rational Bezier curve is defined on [0, 1] by

$$R(t) = \frac{\sum_{i=0}^{n} \binom{n}{i} t^i (1-t)^{n-i} w_i P_i}{\sum_{i=0}^{n} \binom{n}{i} t^i (1-t)^{n-i} P_i}_{i} . \tag{10.2}$$

If the weights are all equal then the rational Bezier curve reduces to the ordinary Bezier curve, since the denominator simplifies to the common weight. Hence only select control points can be "emphasized." An important application of rational quadratic Bezier curves is to the construction of (bits of) conic sections — including circles, ellipses and hyperbolas — without resorting to trigonometric or hyperbolic functions.[79,80]

Now all curves can be in the form of $C(t) = \sum_{i=0}^{n} f_i(t)P_i$, for control points $\boldsymbol{P}_\mathrm{i}$, and basis functions $f_i(t)$. The polynomial interpolation functions can also be realized in this way where the $f_i(t)$ are the well-known Lagrange functions.[79] In the polynomial Bezier case, the $f_i(t)$ are the Bernstein basis functions. It will often happen that $\sum_{i=0}^{n} f_i(t) = 1$ as well, at least on some parameter interval, which ties in with the convex hull property mentioned above when the basis functions are also non-negative.

### 10.4.3. *Elementary surface patches*

The interpolation and Bezier curves can be used to come up with two broad classes of surface patches: tensor product surfaces and lofting surfaces. A surface patch is defined as a function of two parameters $u$, $v$, plotted over some rectangle in the u and v plane, taking values in three spaces. Surfaces of the type $z = \mathrm{f}(x, y)$ can be realized this way, as $\boldsymbol{S}(u, v) = [u, v, (f, u, v)]$.

A tensor product surface patch can be built up from cubic Beziers. Let start with a grid of 16 control points $P_{i,j}(0 \leq i, j \leq 3)$, and then consider the Bernstein functions $3!/i!(3 - i)!u^i(1 - u)^{3-i}$ and $3!/j!(3-j)!v^j(1-v)^{3-j}$, used in the definitions of the cubic Bezier curves controlled by $P_{0,0}, P_{1,0}, P_{2,0}, P_{3,0}$ and $P_{0,0}, P_{0,1}, P_{0,2}, P_{0,3}$, respectively.

We use the set of all possible products of these one variable functions as a basis for our surface: for $u$, $v \in$ belong to $[0, 1]$, define $\mathbf{S}(u, v)$ to be

$$\sum_{i,j=0}^{3} \binom{3}{i}\binom{3}{j} u^i(1-u)^{3-i}v^i(1-v)^{3-i}P_{i,j}. \qquad (10.3)$$

This surface interpolates the corner points $\mathbf{P}_{0,0}$, $\mathbf{P}_{0,3}$, $\mathbf{P}_{3,0}$, and $\mathbf{P}_{3,3}$. Its precise shape may be varied by altering these and the other control points.

A simpler example of a tensor product surface patch is the bilinear surface patch, which also turns out to be the easiest example of the second class of surface patches, lofting surface. Let start with linear Beziers, i.e., straight lines, connecting four points $\mathbf{Q}_{0,0}$, $\mathbf{Q}_{1,0}$, $\mathbf{Q}_{1,1}$,

and $\mathbf{Q}_{0,1}$ (in that order), yielding:

$$Bill(u,v) = (1-u)(1-v)Q_{0,0} + (1-u)vQ_{0,1} + u(1-v)Q_{1,0} + uvQ_{1,1} \tag{10.4}$$

for $u, v \in [0,1]$. This is the simplest surface joining four points. It is a ruled surface, and interpolates the lines which connect the given points.

Replacing the four straight lines in the bilinear surface patch with four curves yields a general curved surface patch. For example, use curves $\mathbf{C}_{u,0}$ and $\mathbf{C}_{u,1}$ joining points $\mathbf{Q}_{0,0}$ to $\mathbf{Q}_{1,0}$ and $\mathbf{Q}_{0,1}$ to $\mathbf{Q}_{1,1}$ and curves $\mathbf{C}_{0,v}$ and $\mathbf{C}_{1,v}$ joining points $\mathbf{Q}_{1,0}$ to $\mathbf{Q}_{1,1}$ and $\mathbf{Q}_{0,0}$ to $\mathbf{Q}_{0,1}$, respectively. A hammock between the curves $\mathbf{C}_{u,0}$ and $\mathbf{C}_{u,1}$ can be obtained by lofting in the $v$ direction. That is

$$Loft_v(u,v) = (1-v)C_{u,0} + vC_{u,1} \tag{10.5}$$

for $u, v \in [0,1]$. This linearly interpolates between corresponding points on each curve.

Similarly, lofting in $u$ direction yields

$$Loft_u(u,v) = (1-u)C_{0,v} + uC_{1,v}. \tag{10.6}$$

The Coons surface construction gives a surface patch which interpolates all four of the space curves. Its parametric equation is given by:

$$Coons(u,v) = Loft_u(u,v) + Loft_v(u,v) - Bil(u,v). \tag{10.7}$$

The Coons surface can be modified by multiplying three component surfaces with three weight factors to form a general form of 3-D surface. This can be used to build 3-D surface of biological morphological surfaces with small features for biomimetics research and development. It is also possible to build various 3-D models by stitching together lofting, Coons, and Bezier patches — or the more general B-spline surfaces or NURBS patches discussed in Sections 10.4.4 and 10.4.5.

## 10.4.4. *B-splines*

B-splines are a class of functions made up of pieces of polynomials, joined together in some fashion. We start by choosing an m+1-tuple $T = [t_0, t_1, \ldots, t_m]$ of non-decreasing real numbers, which is called the

knot vector. We then define the B-splines $B_{i,j}$ of order $j$ recursively, as follows. Set

$$B_{i,1}(t) = \begin{cases} 1 & on\ [t_i, t_{i+1}] \\ 0 & elsewhere \end{cases} \tag{10.8}$$

for $0 \leq i \leq \mathrm{m} - 1$ (with $B_{m-1,1}(t) = 1$ on $[t_{m-1}, t_m]$), and for any $j - m$, we define

$$B_{i,j}(t) = w_{i,j}(t)B_{i,j-1}(t) + (1 - w_{i+1,j}(t))B_{i+1,j-1}(t) \tag{10.9}$$

for $0 \leq i \leq m - j$, where the $w_{i,j}$ is given by

$$w_{i,j}(t) = \begin{cases} \dfrac{(t - t_i)}{(t_{i+j-1} - t_i)} & if\ t_{i+j-1} \neq t_i \\ 0 & otherwise \end{cases}. \tag{10.10}$$

Given $T$ and $k \leq m$, we thus get $m-k+1$ piecewise polynomials $B_{i,k}(t)$ of degree at most $k-1$. The pieces which constitute each function join up at the knots, where they exhibit varying degrees of smoothness.

Order one B-splines $B_{i,1}(t)$ are step functions, order two B-splines $B_{i2k}(t)$ are zig-zag linears, order three B-splines $B_{i,3}(t)$ are piecewise quadratics, and so on.

The multiplicity of a given knot (i.e., how often it is repeated in the knot vector) tells us a lot about the way the pieces of the B-splines join up there: at a knot of multiplicity $l$, each $B_{i,k}(t)$ is at least $k - l - 1$ times continuously differentiable.[79,80] If $k - l - 1 = -1$, this is to be interpreted as a potential discontinuity.

If $k - l - 1 = 0$, this means that the B-splines are continuous but not differentiable, i.e. B-splines have spikes. This feature of B-splines is very useful for building 3-D models of special geometrical features such as tarsus of an insect leg, insect cerci, horn of an ox and filed mouse hair, as shown in Fig. 10.8.

**Fig. 10.8.** Biological surfaces can be 3-D-modelled with B-spline methods by letting $k - l - 1 = 0$. Pictures from http://beetles.source.at/english/anim.htm

#### 10.4.4.1. *B-spline curves*

Given a knot vector $T = [t_0, t_1, \ldots, t_m]$, and the corresponding $m - k + 1$ B-splines $B_{i,k}(t)$ of order $k$, for some fixed $k \leq m$, then if we also have $m-k+1$ control points $\boldsymbol{P}_o, \boldsymbol{P}_1, \ldots, \boldsymbol{P}_{m-k}$, we can put everything together to get a B-spline curve of degree $k-1$ defined on $[t_{k-1}, t_{m-k+1}]$:

$$C(t) = \sum_{i=0}^{m-k+1} B_{i,k}(t) P_i. \tag{10.11}$$

If $T = [0, 0, 0, 1, 1, 1, 1]$ and $k = 4$, we see that C($t$) is just a cubic Bezier curve; indeed any Bezier curve can be realized in a similar way.

#### 10.4.4.2. *B-Spine Surfaces*

The tensor product bi-cubic Bezier surface patch can be generalized to get B-spline surface patches. Let knot vectors $U = [u_0, u_1, \ldots, u_{mu}]$, $V = [v_0, v_1, \ldots, v_{mu}]$, of possibly different lengths, and two curve orders $k_u$; $k_v$. Given a rectangular mesh of $(m_u - k_u + 1)\_(m_v - k_v + 1)$ control points $\mathbf{P}_{i.j}$, we can then define

$$S(u, v) = \sum_{i=0}^{m_u - k_u + 1} \sum_{j=0}^{m_v - k_v + 1} B_{i,k_u}(u) B_{j,k_v}(v) P_{i,j}. \tag{10.12}$$

When both knots vectors are [0; 0; 0; 0; 1; 1; 1; 1] and both orders are 4, we get a bi-cubic Bezier surface patch as seen before.

### 10.4.5. *Non-uniform rational B-splines (NURBS) curve*

Non-uniform rational B-Splines (NURBS)[81] refers to curve and surface generation using not-necessarily uniform (equally spaced) knots in conjunction with the rational function approach already encountered in above discussion of Bezier curves. The NURBS curve is explained in detail by Piegl and Tiller.[82] A $p$th-degree NURBS curve is determined by its control points $\{\mathbf{P}_i\}$, weights $\{w_i\}$, and knots $\{u_i\}$. The polygon formed by the $\{\mathbf{P}_i\}$ is called the control polygon. The knots form a sequence of non-decreasing real numbers while $u_i \leq u_{i+1}$

($i = 0, \ldots, m-1$) and normally $u_0 = \cdots = u_p = 0$, $u_{m-p} = \cdots = u_m = 1$. The number of knots is $m+1$. The $U, U = \{u_0, \ldots, u_p, u_{p+1}, \ldots, u_{m-p-1}, u_{m-p}, \ldots, u_m\}$ is called the knot vector. With the B-spline basis functions $\{N_{i,p}(u)\}$ recursively defined on $U$ as

$$N_{i,0}(u) = \begin{cases} 1 & \textit{if } u_i \le u \le u_{i+1} \\ 0 & \textit{otherwise} \end{cases}$$

$$N_{i,p}(u) = \frac{u - u_i}{u_{i+p} - u_i} N_{i,p-1}(u) + \frac{u_{i+p-1} - u}{u_{i+p-1} - u_{i+1}} N_{i+1,p}(u), \tag{10.13}$$

the NURBS curve is a function of the parameter $u$

$$C(u) = \frac{\sum_{i=0}^{n} N_{i,p}(u) w_i P_i}{\sum_{i=0}^{n} N_{i,p}(u) w_i}. \tag{10.14}$$

It is normally assumed that $w_i > 0$ and $u \in [0, 1]$. The number of control points is $n+1$.

Setting the rational basis functions as

$$R_{i,p}(u) = \frac{N_{i,p}(u) w_i}{\sum_{j=0}^{n} N_{j,p}(u) w_j}, \tag{10.15}$$

where the $\{R_{i,p}(u)\}$ are piecewise rational functions, Eq. (10.14) can be rewritten as

$$C(u) = \sum_{i=0}^{n} R_{i,p}(u) P_i. \tag{10.16}$$

The NURBS curve has many useful and important characteristics. The following presents some characteristics that are related biomimetics research.

(1) $R_{i,p}(\mathrm{u}) = 0$ for $\mathrm{u} \notin [u_i, u_{i+p+1}]$. Therefore, moving a single control point $\mathbf{P}_i$ or changing the weight $w_i$ affects only the segment of the NURBS curve for $\mathrm{u} \notin [u_i, u_{i+p+1}]$, and outside this interval the control point $\mathbf{P}_i$ has no effect. The control points of the NURBS curve are said to exert the property of localness. A complementary fact is that each segment of such curves is controlled by at most $k$ of the $\mathbf{P}_i$'s: the segment between $t_j$ and $t_{j+1}$ is completely determined by $\mathbf{P}_{j-k+1}, \ldots, \mathbf{P}_j$. This is the important property for 3-D-modelling biological surface that requires local modification.

(2) If $u \in [u_i, u_{i+1}]$, then $\mathbf{C}(u)$ lies within the convex hull formed by the control points from $\mathbf{P}_{i-p}$ to $\mathbf{P}_i$. That is the control polygon determines the general shape of the NURBS curve.

(3) All $R_{i,p}(u)$ attain exactly one maximum for all $u \in [0, 1]$ when $p > 0$. When the knot vector reflects the geometric distribution of the control points and all the weights have the same or close values, the maximum values of $R_{i,p}(u)$ generally occur at the curve segment closest to the control point $\mathbf{P}_i$. That is, under the circumstance, the closer a curve point $C(\bar{u})$ is to a control point $\mathbf{P}_i$, the more substantially the modification of the control point $\mathbf{P}_i$ affects the curve point $C(\bar{u})$.

(4) Weight modification has a perspective effect. If a weight $w_i$ changes, each affected point $C(\bar{u})$ will move along a straight line defined by the original point $C(\bar{u})$ and the control point $\mathbf{P}_i$. $C(\bar{u})$ will be pulled toward $\mathbf{P}_i$ if $w_i$ increases, and $C(\bar{u})$ will be pushed away from $\mathbf{P}_i$ if $w_i$ decreases. On the other hand, control point repositioning has a translational effect. That is, when a control point $\mathbf{P}_i$ is repositioned to a new position $\mathbf{P}'_i$, all the affected curve points move in a parallel direction. This property is useful for studying biomimetics limbed robots. For example, for the design and development of jumping robots, it is very important to study the jumping principle and muscle motion of some insects' legs. The 3-D modelling will play an important role. During the 3-D modelling, the control points of the NURBS curves are positioned near the locations where muscles are attached to bones or some locations along the muscles, then the NURBS curves are geometrically associated with a generic polygon mesh representing the muscles. The weights can then be changed or the control points can be repositioned to simulate various motions. These 3-D models can be used not only during the early stage performance analysis and biomimetics design, but also for manufacturing at late stage.

(5) The two knots which are closer together seem to be dragging the curve towards the control point. The double knot can be used to obtain an interpolation of one of the control points. This property can be used to build 3-D models of biological features with small round corner by sneaking the two knots up on a knot from the both sides.

The above features should be further exploited for the 3-D model building of biological surfaces for biomimetics.

### 10.4.6. *NURBS surfaces*

If we extend one dimensional parameter space ($u$) in NURBS curve to two dimensional parameter space ($u, v$), we get NURBS surface. A non-uniform rational B-spline surface of degree ($p, q$) is defined by

$$\mathbf{S}(u, v) = \frac{\sum_{i=0}^{m} \sum_{j=0}^{n} N_{i,p}(u) N_{j,q}(v) w_{i,j} \mathbf{P}_{i,j}}{\sum_{i=0}^{m} \sum_{j=0}^{n} N_{i,p}(u) N_{j,q}(v) w_{i,j}}, \tag{10.17}$$

Similarly, the property analysis for NURBS surface should be done for the 3-D model building of biological surfaces for biomimetics.

## 10.5. Applications of 3-D Modelling in Biomimetics

### 10.5.1. *An innovative methodology of product design from nature*[83]

#### 10.5.1.1. *Introduction*

Nature is an information sourcebook for behavior, function, color and shape, which can inspire visual design and invention. Studying the form and functional characteristics of a natural object can provide inspiration for product design and help to improve the marketability of manufactured products. The inspiration can be triggered either by direct observation or captured with three-dimensional (3-D) digitizing techniques to obtain superficial information (geometry and color). An art designer often creates a concept in the form of a two-dimensional (2-D) sketch while engineering methods lead to a point cloud in 3-D. Each has its limitations in that the art designer commonly lacks the knowledge to build a final product from a 2-D sketch and the engineering designer's 3-D point clouds may not be very beautiful. In this section, an innovative methodology of product design from nature will be presented for Product Design from Nature (PDN), coupling aesthetic intent and geometrical characteristics, exploring the

interactions between designers and nature's systems in PDN. It was believed that this approach would considerably reduce the lead time and cost of product design and development from nature.

### 10.5.1.2. *Discussion of bio inspiration of product design*

In 1984 Nigel Cross published *Developments in Design Methodology*, collecting influential articles about methods and procedures over the past two decades. His book reflected developments in the design research community. The approach was defined as ". . .the study of how designers work and think; the establishment of appropriate structures for the design process; the development and application of new design methods, techniques and procedures; and reflection on the nature and extent of design knowledge and its application to design problems."[84]

Conceptual design is normally optimized by iteration due to the lack of ideas at the early stage of design. The iteration process is very time-consuming and expensive, returning to earlier stages to modify the designers' ideas, often resulting in long lead time and high cost of introducing a new product onto the market. Moreover, the design philosophy of "form follows function" is no longer sufficient; the aesthetic aspect of a product has become a more and more important element for success. In addition, the shift in manufacturing paradigm will have a deep impact on design and operation of future manufacturing systems.

The development of computer-based design has given rise to beguiling but rather rigid images, and this in turn has caused researchers such as Soufi and Edmonds to observe that "current computer aided design (CAD) systems do not provide sufficient support to the early conceptual stages of design."[85] For designers, it is important to understand how invention works in design, and where and how it breaks down. One of the inventive processes is conceptual design where inspiration and observation can arise or be learned from nature. This is called the conceptual design process "Product Design from Nature" (PDN).

The inspiration from a natural system is called bio-inspiration. Bio-inspiration can be triggered either by direct observation by an art design professional or captured by an engineering designer using

3-D digitizing techniques to obtain surface information. An art design professional often creates a conceptual design in the form of a 2-D sketch while the engineering method leads to a point cloud in 3-D. Both methods are limited: the art design professional lacks the knowledge to build a final product from a 2-D sketch and the engineering designer's 3-D point clouds are not very aesthetic. In this methodology, the proposed method for product design integrates reverse engineering, 3-D geometrical computation and inspiration from a designer's sketch of biological systems for conceptual and form design and form aesthetics.

It is common to look to nature for inspiration,[2,4,86] but there are few instances of successful transfer of the technology into design. The fundamental issues are to understand (1) the behavior and function of the natural system; (2) how natural systems perform their functions and their physical, chemical and biological properties; (3) the designer's observation captured in the freehand sketch; (4) geometrical characterization of natural systems including 2-D and 3-D models, a joint effort of engineering and graphic design, which leads to the final conceptual design based on functional requirements and form aesthetics; and (5) the design of a prototype and its development by testing. Of these, geometrical features, the designer's sketched inspiration, and the form aesthetics of natural systems are essential for designing a bionic product.

### 10.5.1.3. *Proposition of a methodology for PDN*

There are normally two methods for capturing geometric information for bio-inspiration. First, art design, in which the direct observation of a natural object is undertaken by art design professionals with their special knowledge and experience. Second, the engineering method, in which engineers measure a natural object using methods such as reverse engineering. Both methods have their advantages and disadvantages. The PDN method aims to combine the advantages of both methods and overcome the disadvantages of each (see Fig. 10.9).

The procedure is as follows:

*Stage 1 — Capturing surface geometrical information*

A professional designer observes a biological object such as an apple, a lotus leaf or a bird to get bio-inspiration. With their expert knowledge,

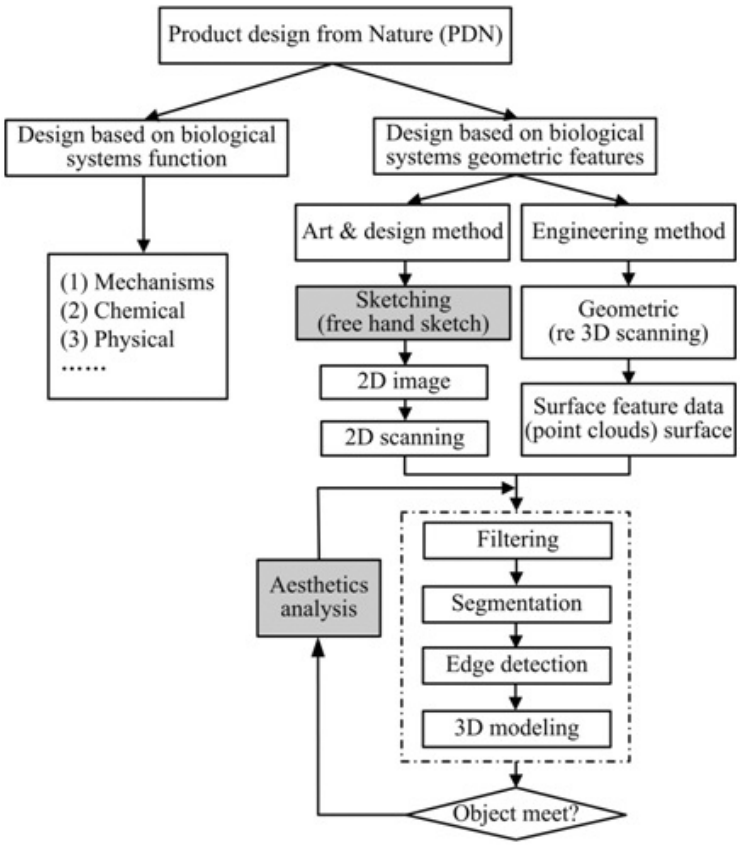


**Fig. 10.9.** The proposed methodology for PDN.

experience and talent, they use their imagination to design either a pre-defined product or something totally new. The output is usually a 2-D sketch (freehand drawing) which can be scanned to get digitized geometrical information in a format suitable for later processing to generate the geometrical information required for 3-D models using the algorithms in Stage 2. Alternatively, an engineer measures geometrical and color data directly from a natural object. The outputs are normally various sets of points in x-, y- and z-coordinates for geometrical data and r, g and b for color. These are "point clouds" which can be processed to generate information for geometrical design

(such as 3-D models) and aesthetic design using various algorithms in Stage 2.

*Stage 2 — Building a 3-D model*

This consists of filtering, segmentation, edge detection, and initial 3-D modelling, iterative analysis/optimization for the final 3-D models, considering also the aesthetics. There should be sufficient collaboration between professional designers, engineers and 3-D modelers. The inputs from designers should be effectively integrated into 3-D modelling to retain aesthetic beauty in the designed product. The inputs from engineering design and the 3-D modeler are used to build 3-D models that are suitable for production in Stage 3. In this stage, various algorithms have to be applied.

*Stage 3 — Manufacturing a prototype*

The aim of any product design including PDN is to provide a description for manufacturing a physical product. This is important for bionic engineering to be successfully integrated into the development and manufacturing process. So the natural stage of the proposed method should be to build some prototypes for testing, quality control and production of the product for market. Various rapid prototyping techniques/methods are available commercially. Typical methods include rapid prototyping, high-speed machining, laser cutting and processing, etc.[86]

The innovation is in the integration of art design with engineering design for PDN. A number of algorithms have to be used. Some of them have been developed, but some of them still need to be developed. The details of the procedures of art design direct observation — sketching from a natural object — can be found in Ref. 83.

#### 10.5.1.4. *A case study of the design of light shade — learning from lotus leaves*

In this sub-section, a case study is presented to demonstrate how to follow the proposed methodology to design a light shade by learning from lotus leaves.

Figure 10.10 shows a 2-D sketch by an art design professional based on bio-inspiration after observing a lotus plant. This sketch

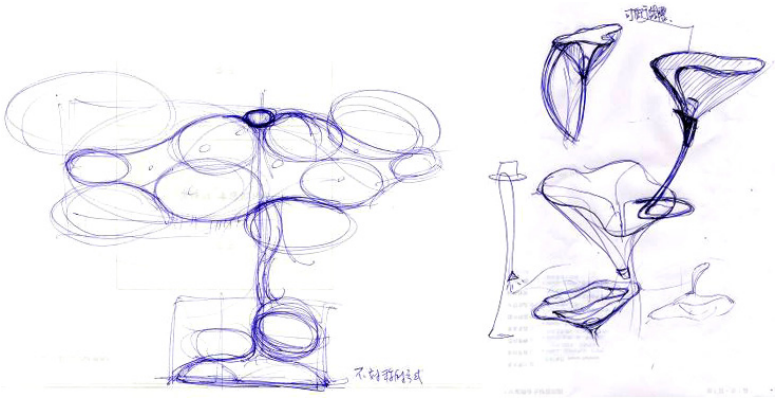

**Fig. 10.10.** A 2-D sketch based on the bio-inspiration.[83]

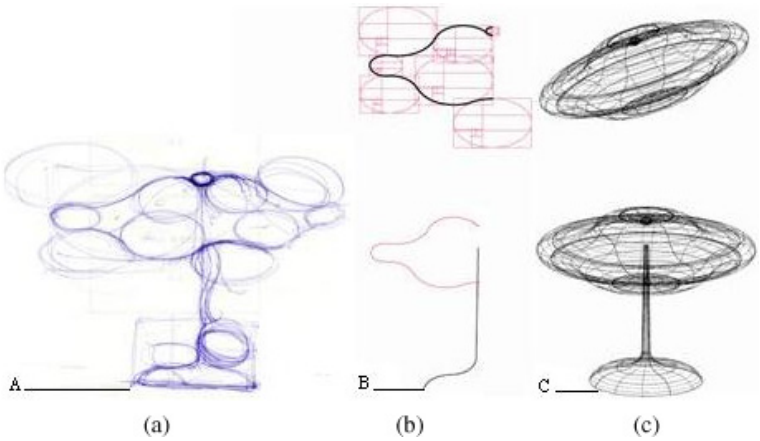


**Fig. 10.11.** (a) sketch, (b) curves; (c) 3-D model.[83]

can be processed through scanning, sampling, edge detection and segmentation to generate curves/surfaces (Fig. 10.11) which can be used to build a 3-D wire frame model (Fig. 10.12). This 3-D model can be further modified to generate the final 3-D model and design specification — PDN. The final design can be used for a prototype, as shown in Fig. 10.13. This prototype was produced using 3-D printing.

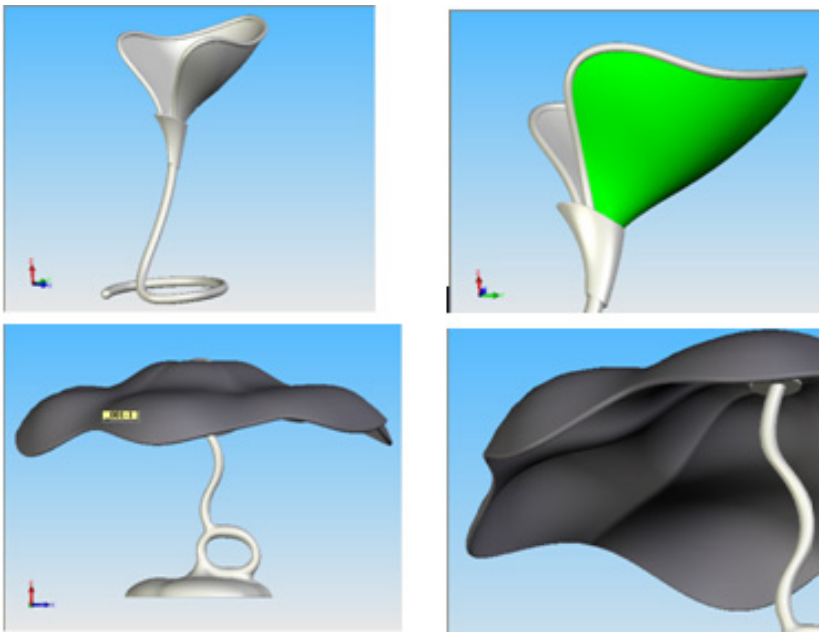

**Fig. 10.12.** 3-D models.[83]

**Fig. 10.13.** Prototype.[83]

### 10.5.1.5. *Summary*

The proposed methodology is a method for innovative product design from nature, coupling aesthetic intent and geometrical characteristics,

exploring the interaction between designers and nature systems in product design from nature. From the case study, it can be seen that the method is valid and useful for designers to do innovative design by learning from nature.

However, the methodology needs to be further developed before it can be used in real product design from nature. In particular, great efforts have to be made on how to design and develop an effective and efficient algorithm to build a 3-D model from a designer's 2-D sketches and how to design and develop a computer system that is either workstation-based or web-based (though web-based is preferable) as a platform for both art designers and design engineers to effectively collaborate during the optimization of the design and aesthetics to increase the marketability of the products.

## 10.5.2. *A new parameterized feature-based generic 3-D human face model for emotional bio-robots*[87]

### 10.5.2.1. *Introduction*

Emotional bio-robots are one of the important areas of bionic robots applications. To represent human facial expressions is an essential requirement for building emotional bio-robots because the expressions can help bio-robots communicate with human beings emotionally. To design and develop emotional robots, it is necessary to build a generic 3-D human face model. While the geometrical features of human faces are freeform surfaces with complex properties, it is the fundamental requirement for the model to have the ability of representing both primitive and freeform surfaces. This requirement makes Non-rational Uniform B-Spline (NURBS) suitable for 3-D human face modelling.

In this sub-section, a new parameterized feature-based generic 3-D human face model is presented and implemented. Based on observation of human face anatomy, the model defines 34 NURBS curve features and 21 NURBS surface features to represent the human facial components, such as eyebrows, eyes, nose and mouth, *etc*. These curve models and surface models can be used to simulate different

facial expressions by manipulating the control points of those NURBS features. Unlike the existing individual-based face modelling methods, this parameterized 3-D face model also gives users the ability to use the model to imitate any facial appearances. In addition, the potential applications of the new proposed 3-D face model are also discussed. Besides emotional bio-robots, it is believed that the proposed model can also be applied in other fields such as aesthetic plastic surgery simulation, film and computer game characters creation, and criminal investigation and prevention.

#### 10.5.2.2. *Discussion of the methods for human face 3-D models*

With the rapid development and application of 3-D modelling techniques, a lot of research has been carried out to study human faces and to build 3-D face models for various applications,[88–90] especially for emotional bio-robots, aesthetic surgery, crime detection and computer games, etc. One intuitive approach to modelling human faces is using scanned 3-D data. It is a type of active stereo vision method. The data obtained using 3-D scanners — so-called "clouds" — is a complete set of 3-D information including 3-D coordinates, colors, and textures rather than the profile images of an object. The number of points in "clouds" varies from hundreds of thousands to millions. Based on these "clouds," different algorithms are developed to build the corresponding 3-D models.[91–94]

Another 3-D modelling method is the triangular patches method, which is a surface approximation method. Although each triangle can be expressed in a 2-D plane, numerous triangles in 3-D can be connected together to approximate an arbitrary surface. A famous triangular patches face model is CANDIDE,[95] which uses hundreds of triangles to represent a 3-D human face with several simple facial features. Since the first CANDIDE model was proposed, several variations have been proposed.[96–98]

The third approach of modelling 3-D human faces is the statistical model-based method. The most successful statistical face model is the morphable model established by Blanz and Vetter.[99] A pixel-level 3-D prototype face database was constructed to store the statistical data. A

morphable face model was derived by transforming shape and texture into a vector space representation. Later, other researchers proposed various modelling methods based on 3-D morphable model using collected statistical scanning data sets.[100–102]

Even though there are several existing modelling methods, the gap between these methods and the requirements of emotional bio-robots applications still urges the creation of a parameterized generic 3-D human face model:

- First of all, human faces consist of a number of geometrical regions which contain different muscles under the skin. The expressions are too complicated to simulate with a single surface model because even the minor expressions involve multiple muscles. Difficulties also exist in transferring expressions of one bio-robot to another because there is no parametric representation of the face models.
- Second, the 3-D face model required by emotional bio-robots should be capable of generating faces with arbitrary appearances through manipulating the facial features. The previous modelling methods only provide mechanisms to represent a 3-D face from data points.[96,103] They were not mainly designed for representing facial features and especially their boundary information. Another approach for 3-D face modelling is for professional engineers to design the model using 3-D modelling software. But the accuracy will depend on the experience of the engineers. It is not easy for an ordinary person to create a face model.
- Third, sometimes the target people cannot present for scanning — even an image of the target person is difficult to obtain in some cases. For example, the clear frontal images of terrorists are rarely circulated in ordinary circumstances. So it is not feasible to build 3-D face models using existing modelling methods.

From the above discussions, it can be seen that it is necessary to develop a parameterized generic 3-D face model that can be used to help the engineers design and develop emotional bio-robots even when the robots' faces are not similar to any existing human beings, because the appearances of the robots can be easily changed by morphing some facial features of the generic model.

In this model, techniques of NURBS will be used. Details of NURBS can be found in Section 10.4 or from Ref. 87.

#### 10.5.2.3. *Face model definition*

To build up a parameterized generic 3-D face model, a human face should be divided into a number of geometrical surfaces for the purpose of expressing the whole face with features-based parameterized geometrical models. Based on the features analysis (such as nose, mouth, eyes and chin, etc.) on a human face[104,105] and the convenience and effectiveness of manipulating the generic 3-D model, 34 curve features are defined on a human face (as shown in Fig. 10.14). These curve features can be combined together to form 21 surface features (as shown in Fig. 10.15).

#### 10.5.2.4. *Reverse computation and 3-D manipulation of facial features*

As soon as all facial features are defined, they need to be manipulated to change the appearance of the model, and the adjacent features are connected together, which means no holes and gaps on the surface model. In practice, the degree of NURBS curve and surface is usually chosen as 3 to get a balance between control flexibility and computation complexity.[106] All weights are set to 1 initially and can be adjusted while manipulating the models. So the next step is to calculate NURBS control points and knot vectors by reverse computation.

The problem of NURBS curve reverse computation can be described as: Given a set of data points $Q = \{q_0 q_1 q_2 \dots q_m$, to compute the control points $\mathbf{P}_i$, weights$w_i$, and knot vector $\boldsymbol{U}$ with a specified degree $p$ which starts from $q_0$ ends with $q_m$, and passes through $q_2$ to $q_{m-1}$. The problem of NURBS surface reverse computation is similar except it is described in a 3-D space.

Assume $\mathbf{U} = \{u_0 u_1 u_2 \dots u_{n+1} u_{n+2}, \dots u_{n+p} u_{n+p+1}$ is the knot vector of target NURBS curve, because the NURBS curve passes through the first and last control points, such condition for knots holds: $u_0 = u_1 = u_2 = \cdots = u_p = 0$, $u_{n+1} = n_{n+2} = u_{n+3} = \cdots = u_{n+p+1} = 1$. Only the knots between $u_{p+1}$ and $u_n$ are unknown. Because

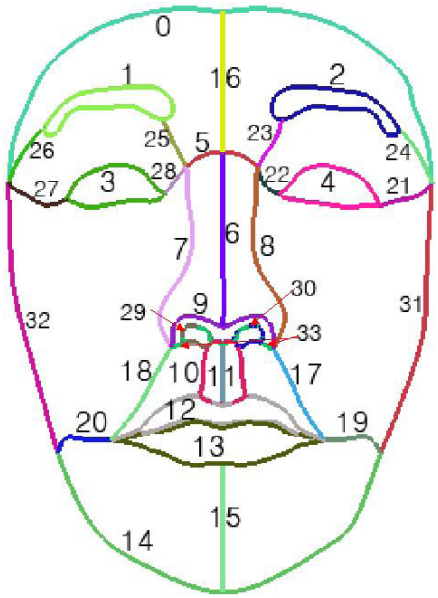


**Fig. 10.14.** Features of NURBS curve face model.

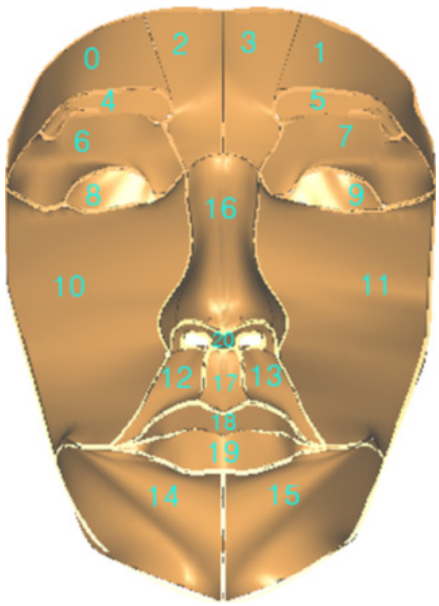


**Fig. 10.15.** Features of NURBS surface model.

the clamped NURBS passes through the first and last control points, these two points are set as duplicated control points in this paper. The relationship between the number of control points $n$ and the number of data points $m$ is $n = m + 2$. So the total number of knots in knot vector is $n + p + 1 = m + 2 + 3 + 1 = m + 6$, and the total number of control points is $n+1 = m+3$. The unknown knots in the knot vector from $u_{p+1}$ to $u_{m+2}$ $(u_n)$ can be computed by parameterizing knots for each data point $q_j$. As expressed in Eq. (10.18), the cumulative chord length method[107] is used to calculate all knots:

$$\begin{aligned} u_0 = u_1 = u_2 = u_3 = 0 \\ u_{i+3} = u_{i+2} + \frac{|q_i - q_{i-1}|}{\sum_{i=1}^{m} |q_i - q_{i-1}|} \quad \text{for } i = 1, 2, \ldots, m-1 \\ u_{m+3} = u_{m+4} = u_{m+5} = u_{m+6} = 1. \end{aligned} \tag{10.18}$$

The target curve will pass through all $m$ data point $q_i$ $(0 \leq i \leq m)$, which means $m+1$ equations can be obtained according to Eq. (10.19). But according to the analysis above, the target NURBS curve has $m + 3$ control points. The target NURBS curve is tangent to the bounding polygon at the first and last control points. This introduces two boundary conditions.

$$\begin{aligned} j = \boldsymbol{C}(u) &= \sum_{j=0}^{m} \boldsymbol{N}_{j,p}(\bar{u}_j)\boldsymbol{P}_j \\ &= \sum_{j=0}^{m} \boldsymbol{N}_{j,3}(\bar{u}_j)\boldsymbol{P}_j \quad (j = 0, 1, 2, \ldots, m) \end{aligned} \tag{10.19}$$

Using these two boundary conditions and parameterized knot vector, the linear equation of $\boldsymbol{AP} = \boldsymbol{D}$ are generated as Eq. (10.20).

$$\begin{bmatrix} a_0 & b_0 & c_0 & \cdots & \cdots & \cdots \\ a_1 & b_1 & c_1 & \cdots & \cdots & \cdots \\ \ddots & \ddots & \ddots & \cdots & \cdots & \cdots \\ \cdots & \cdots & a_{m+1} & b_{m+1} & c_{m+1} & \cdots \\ \cdots & \cdots & a_{m+2} & b_{m+2} & c_{m+2} & \cdots \end{bmatrix} \begin{bmatrix} P_0 \\ P_1 \\ \vdots \\ P_{m+1} \\ P_{m+2} \end{bmatrix} = \begin{bmatrix} d_0 \\ d_1 \\ \vdots \\ d_{m+1} \\ d_{m+2} \end{bmatrix} \tag{10.20}$$

Where $d_0$ and $d_{m+2}$ are the bounding conditions at the first and last control point, $d_j = q_{j-1}$ for $j = 1, 2, \ldots, m+1$, and $a_i$, $b_i$, $c_i$ for

$i = 1, 2, \ldots, m+1$ are the basis functions of three degrees for each $\boldsymbol{u_i}$ previously computed using the cumulative chord length function. The control points vector $\boldsymbol{P}$ can be computed by $\boldsymbol{P} = \boldsymbol{A}^{-1}\boldsymbol{D}$.

As the degree, knot vector, and control points of the NURBS curve are computed, the unique curve can be evaluated using the de Boor[108] algorithm. It can also be considered as the NURBS curve whose weights equal one. It can be changed freely by either control points or weights factors. Figure 10.16 is an example of the reverse computation.

By extending the above method to 3-D space, it is easy to get the NURBS surface reverse computation. First, all boundaries of the target surface are computed using NURBS curve reverse computation. Next, the knot insertion is performed to make sure each pair of opposite boundaries has the same number of knots. Then, the "control net" (matrix of control points) of the target NURBS surface is determined by interpolating between each pair of control points on the opposite boundaries. Finally, the surface can be evaluated according to computed knots and control net. Figure 10.17 is an example of NURBS surface reverse computation of the nose feature. By applying the reverse

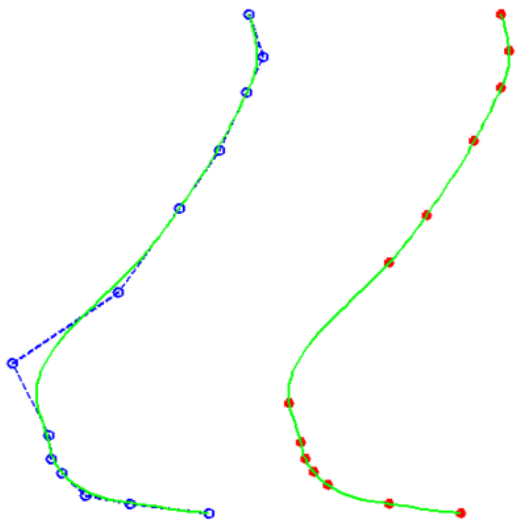

**Fig. 10.16.** NURBS curve by reverse computation. Left: calculated control points; Right: original data points.

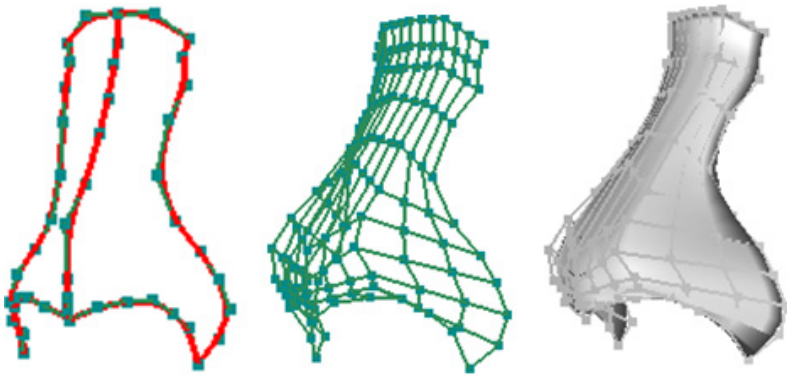

**Fig. 10.17.** Nose surface reverse computation. Left: boundary NURBS curves; Middle: computed control net; Right: evaluated NURBS surface.

computation for all defined features, the NURBS surface face model can be constructed.

### 10.5.2.5. *Experiment results*

To verify the proposed model, a generic parameterized feature based 3-D human face model is implemented in VC++.NET environment. The constructed generic 3-D face models are vivid and intuitive with defined adjustable features. Figures 10.18 to 10.21 illustrate the abilities of morphing facial features of the proposed curve and surface face models. According to the simulation, the features of the proposed models are

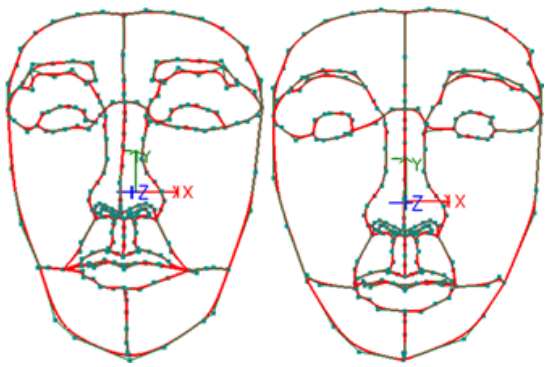

**Fig. 10.18.** Generic and morphed curve face models.

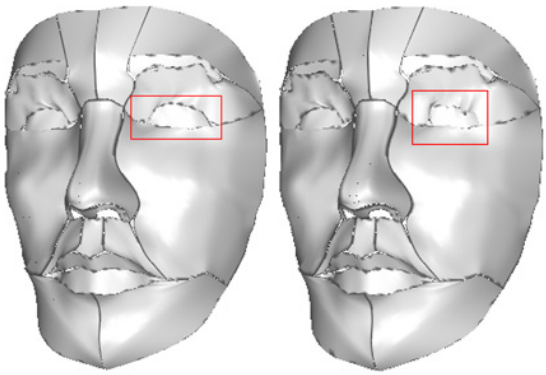

**Fig. 10.19.** Original surface model and model with morphed left eye.

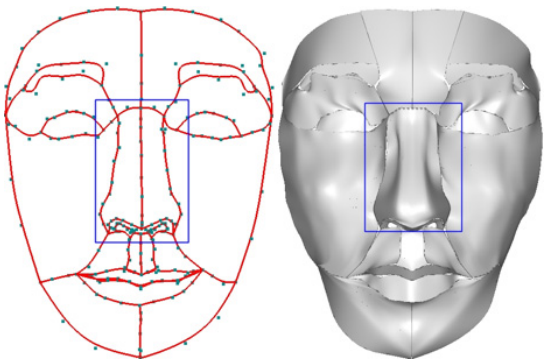

**Fig. 10.20.** Curve face model and surface face model with wider nose.

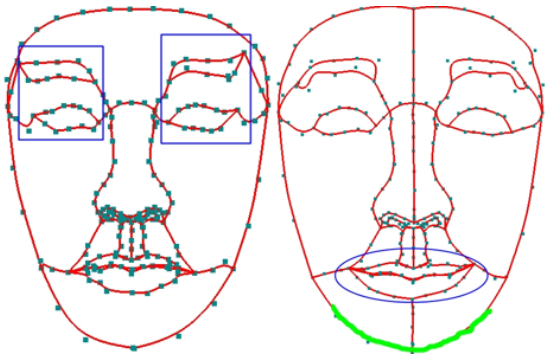

**Fig. 10.21.** Morphed NURBS curve face model. Eyes and eye brows in different shapes (left). Smiling mouth and morphed under jaw line (right).

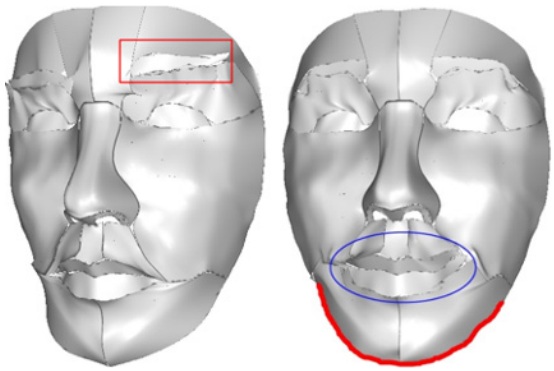

**Fig. 10.22.** Morphed NURBS surface face model. Right brow in different shape (left). Smiling mouth and morphed under jaw line (right).

flexible and can be manipulated to represent various appearances or different facial expressions.

#### 10.5.2.6. *Summary*

The method proposed can be used to build a parameterized generic 3-D human face model with NURBS curves and surface features by applying reverse computation to data points. By comparing the new proposed model with other existing 3-D modelling methods, this parameterized face model can represent the real 3-D surface of a human face mathematically to provide flexible control over all facial features. The feature-based approach is very useful for performing manipulation on all defined facial features to represent various facial expressions. By combining with a face detection method,[109] it is possible to generate the 3-D face model from images of a person automatically, which can potentially be applied in the field of face aesthetics surgery and crime prevention.

### 10.5.3. *3-D geometry modelling of porous copper materials*

#### 10.5.3.1. *Introduction*

This sub-section presents a method for generating 3-D geometrical modelling of porous materials. This method can be applied to build

3-D model of human bones. The procedure of the method will be presented and some examples of 3-D models of porous copper will also be presented.

### 10.5.3.2. *The procedure of the suggested method*

The geometrical characteristics of porous materials are that the size of the pores is very small compared with the body size of the materials (or components). For example, the pore size of a sandstone is a few microns. There are a number of previous methods for modelling such porous materials.[110–111] However, these methods are not suitable for building 3-D models of porous metals with pore size from 20 to 600 microns, especially when the distribution is not as even as that of natural sandstones. So it is necessary to propose and develop a method for building 3-D models of porous metals.

The principle of the proposed method is to slice the materials, get the 2-D geometrical information (boundaries) of the pores found on each slice and join all found boundaries of each pore in all slices to build 3-D models.

There are nine steps in the proposed method. The procedure is as follows:

(1) Determine the number of slices and thickness of each slice.
(2) Mill the porous materials from the selected height to the required height to obtain a number of slices. The number of slices can be determined based on the application requirement. Due to the large number of the pores in each slice, it is not necessary to have a large number of slices. The height of each slice can be determined based on the application requirement and the material production.
(3) Use a selected microscope to scan the surface of each slice to collect the geometrical information of the cross-sections of all pores in each slice. It should be pointed out that multi-scanning is required to cover the whole surface area for each slice.
(4) Merge the images scanned in Step 3 to generate a single image for each slice.
(5) Find the boundaries (x- y- and z-coordinates) of cross-sections of all pores in each slice. Repeat the process to obtain the boundaries of all pores in all slices.

(6) Input the identified cross-section boundaries into CAD software to generate 3-D models for all pores in the materials.
(7) Build a 3-D solid model of the same size of the porous materials.
(8) Use Boolean operation functions in CAD software to generate a 3-D model of the porous materials.
(9) The 3-D model generated in Step 8 can be used as the basis model for generating the 3-D model of a product of porous materials. It should be pointed out that the product can be of any required geometrical size and shape. Hence the method can be used to generate any required 3-D model. So this study will not provide a generic geometrical model of a given porous material, but a generic method for building 3-D geometrical models of any product design.

#### 10.5.3.3. *Case study of 3-D modelling of porous copper*

A sample of porous copper was selected for 3-D modelling.

**(1) Determine the number of slices and thickness of the slice**

The pore distribution of the selected porous copper repeats every 200 microns in height. So in theory, it is reasonable to slice the material to a 200 micron height to obtain the geometrical information for building the 3-D model. However, to increase the reliability and to balance the amount of test work, it was decided that the number of slices of the first copper sample is 60 and thickness of each slice is 100 microns. So the total height of the test is 6,000 microns (6 mm). The images of these 60 slices can be evaluated to find high-quality ones for 3-D modelling.

**(2) Mill the porous materials from the selected height to the required height to obtain the slices**

It is very important to use a milling machine with the required accuracy. A CNC milling machine was used — a LEADWELL V-30 vertical CNC made in Taiwan, and the controller is a FANUC Series 21-M and the CNC system milling error is 0.002mm. A new cutter was used. The cutter's diameter is 2 cm to make sure the cross-section can be milled in one go. From the observation of the milled surface, there are no clear forced deformations found. That means the CNC milling method is suitable for the test.

**Fig. 10.23.** Zeiss SteREO Discovery V20 microscope.

**(3) Scan the surface of each slice to collect the geometrical information of the cross-section of all pores for each slice**

It was decided to use a microscope to capture the image of the cross-sections. A Carl Zeiss SteREO Discovery V20 was used, as shown in Fig. 10.23. As discussed above, multi-scanning is required to cover the whole surface area for each slice. Based on the measurement of the sizes of pores on each cross-section, the magnifier factor of 20 was selected as a compromise between the clearness of the images and the number of images. For the sample, 20 images are required to cover the whole cross section area. A typical image is shown in Fig. 10.24.

**(4) Merge the images scanned in Step 3 to generate a single image for each slice**

After a few trials, it was found that Microsoft painter is a convenient and reliable software to merge images scanned in Step 3 to generate a single image for each slice. Every effort has to be made to ensure that all individual images of each slice are accurately merged into a single one. There are some overlaps between images. The same pore features in the overlaps of the images are identified as the reference for merging. This work could be done by developing a Matlab program.

**Fig. 10.24.** A typical image captured using the microscope.

### (5) Identify the boundaries (x- and y-coordinates) of cross-sections of all pores in each slice

Considering the requirements of 3-D modelling and the time needed, 11 slices of the sample with high image quality were selected for further geometrical information processing (the identification of boundaries of pores, their 3-D modelling and pore sizes and distribution analysis). A method has been developed using some functions of Matlab's artificial intelligent tool box and a few self-developed algorithms for the boundary identification. Figure 10.25 shows the found boundaries of pores for one typical slice. This kind of jpg file can be properly viewed using free software such as Windows Photo Gallery.

During this process, the data of x- and y-components of all pores in each slice was recorded in a single data file in a neutral file format. They can be inputted into any software. The z-component of each point on identified boundaries can be added using software like Excel.

### (6) Input the identified cross-section boundaries into CAD software to generate 3-D models for all pores in each slice

SolidWorks CAD was selected for building the 3-D models of the porous materials. Since the x-, y- and z-components of all points of all pores in each slice are saved in a single file, when this data file is loaded into SolidWorks, the software treats the whole file as a single point

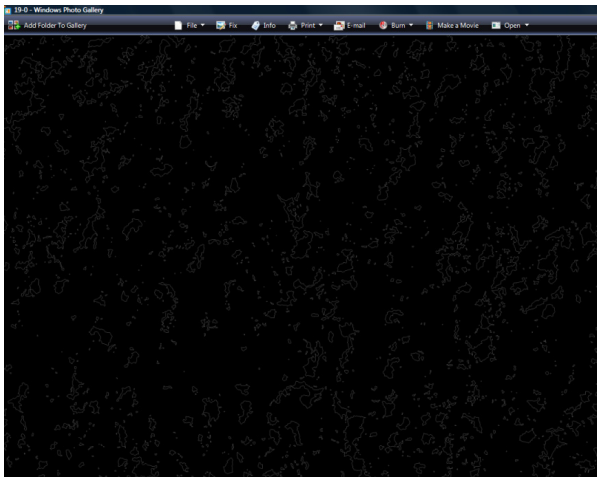

**Fig. 10.25.** Identified the boundaries of all pores.

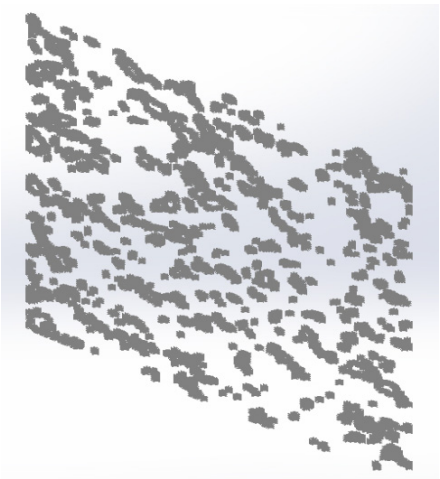

**Fig. 10.26.** Point cloud in SolidWorks (whole slice).

cloud, as shown in Fig. 10.26. A macro was written in the SolidWorks environment, and this macro can be used to load the data file for each slice into the SolidWorks environment and automatically process the data file to identify all points for each pore and to build curve models of all pores in each slice. After running this macro, all curve

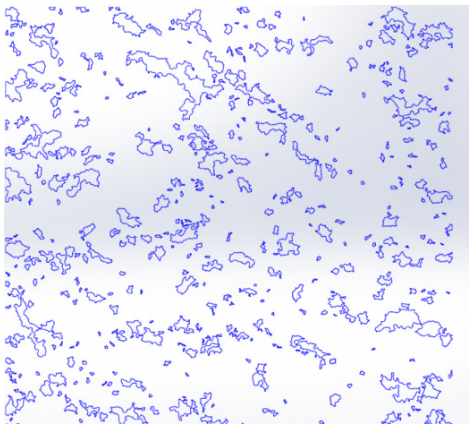

**Fig. 10.27.** Curve model of pores in a typical slice.

models for each slice are generated and saved in a single file, and these curve models can be separately selected for solid modelling, as shown in Fig. 10.27.

**(7) Solid modelling of pores in each slice**

The curve models generated in (6) were used for 3-D solid modelling of pores, as shown in Fig. 10.28. It was noticed that due to the large number of pores and irregularity of the pore shapes of a typical porous copper, the file sizes of 3-D models of porous materials can be very large. For example, the file size of a 3-D solid model of each slice of this sample is about 100 MB. So it would be advisable to generate a 3-D model of a small piece. This model can be used to build the 3-D model of the real product. The 3-D solid model of a typical slice is shown in Fig. 10.29.

### 10.5.3.4. *Summary*

A method for generating 3-D models of porous materials has been described. The experiment results show that the proposed method can be used to build a 3-D model of the porous materials with a large range of pore sizes and vey irregular pore shapes. However, this is a time-consuming process. More work should be done to make the process as automated as possible to reduce the time required for 3-D modelling of porous metals.

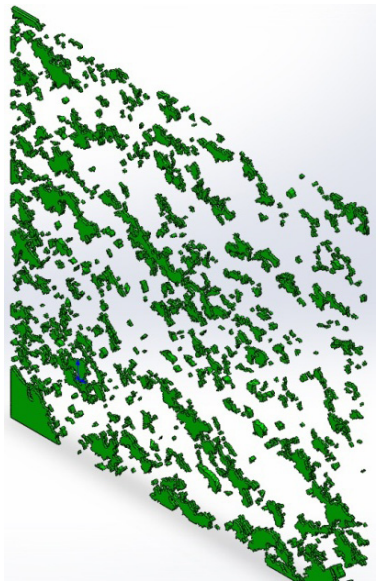

**Fig. 10.28.** 3-D solid model of pores in a typical slice.

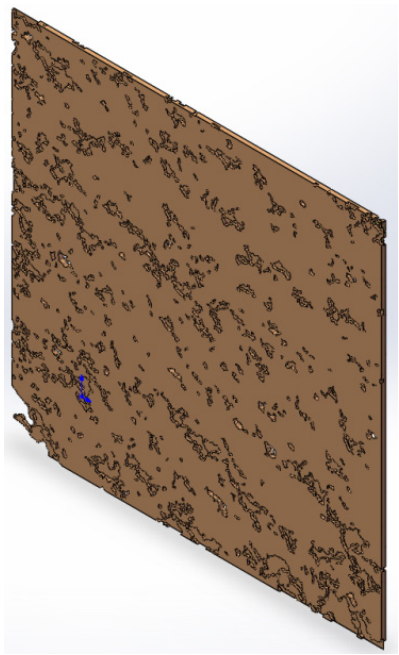

**Fig. 10.29.** 3-D solid model of a typical slice.

## 10.6. Discussion of Problems and Future Research Interests Areas

As discussed above, there have been many different kinds of 3-D modelling techniques and systems available on the market. They can be applied to biomimetics research based on their accuracy, resolution, operationability, cost and efficiency, etc. However, they have been designed mainly for industrial, medical and animation applications. So there are various limitations when they are directly applied to biomimetics research and applications. This section will discuss these limitations and try to list future research areas in 3-D geometrical modelling of animal, insects and plants for biomimetics.

### 10.6.1. *Limitations of existing 3-D systems*

The main limitations of the most existing 3-D geometrical modelling systems are:

#### 10.6.1.1. *3-D Scanners*

(1) The ranges of the accuracies and resolutions of most industrial 3-D scanners are not wide enough to meet all the requirements of biomimetics research and applications. The typical accuracy and resolution are within the range of 25 $\mu m$ to 200 $\mu m$. 3-D geometrical modelling of many biological surfaces needs the accuracy to be as high as from 0.5 $\mu m$ to 10 $\mu m$ and the resolution as high as 0.2 $\mu m$ *to* 1$\mu m$ to secure the accurate geometrical descriptions and acquisition of critical geometrical information at local areas such as sharp tip points of insect tarsus, boundary of convex spherical types of tiny features on the forehead of the female dung beetle. The accuracy of some industrial CMM (co-ordinate measuring machines) can be as high as $\leq$1 $\mu m$, but this accuracy is for single-dimensional measurement, not for area scanning, and the environment conditions are very strict.

(2) Though they have high accuracy and resolution, the workable ranges/areas/spaces are not large enough for most scanners developed for nano-technology study and medical applications.

The effective scanning area is typically within several square *mm* for one setting, so it is very difficult to use this kind of scanner to capture surface geometrical information. If doing multi-scanning, the point clouds alignment or image connection will bring in errors, which makes the whole process low accuracy.

(3) The measurement platform is not flexible enough for capturing complex body geometry of biological objects. The sample table/platform/bed of most scanners with high accuracy and resolution are fixed horizontally or with very limited mobility (Renishaw, Zeus, MicroScope, MRI, etc). To achieve complete data acquisition, extra fixtures have to be used on the table to allow the biological body to be moved to the required positions and orientations. So, the fixtures have to be very accurate, which leads to either long time delay or unbearable costs. This is especially true for a single scanning of an individual surface, which is mostly the case in biomimetics research.

#### 10.6.1.2. *Raw data pre-processing*

(1) Noise filtering — 3-D modelling software provides modules for noise filtering. However, the function is very limited and manual operations have to be included to get a "clean" point cloud suitable for the late processing and modelling operation. This could be a big potential problem for 3-D biological body modelling since morphological surfaces of biological bodies are rarely regular primitives, even not smooth. Actually, one of the promising areas in biomimetics is the study of geometrically non-smooth features of biological systems to design man-made systems with high performances such as the non-smooth surface of some fighters, non-smooth earth-moving components and low-water-resistance swimming suits. To design and produce morphological non-smooth systems, it is necessary to have an accurate description of geometrical non-smooth features of the biological body. These features are normally in very small scale and in large number. The noise filtering of such a point cloud is very challenging. As far as the authors are aware, there isn't any commercial software that is suitable for this task.

(2) Sampling — Sampling techniques are relatively more mature than those for edge detection and segmentation. However, most sampling algorithms were developed for industrial and medical and small-scale non-biotechnology applications. So they are not functionally sufficient and efficiently high enough for 3-D geometrical modelling in biomimetics research. For example, it is really a challenge to sample a point cloud of a non-smooth surface of a biological body, as discussed in 1), so that the sampled point cloud has the desired point distribution of high density along edges/boundaries areas and low density away from edges.

#### 10.6.1.3. *Segmentation and edge detection*

(1) Edge detection is one of most desired techniques in reverse engineering. Unfortunately, there have not been reports of fully reliable software for autonomous edge detection, though efforts have never been stopped.[54–56]
(2) There is also no reliable autonomous software segmentation, especially for point clouds, though a considerable amount of work has been done.[56] It is very important to properly segment the point cloud of a biological body into sub-clouds so that each sub-cloud represents just a unique feature that is suitable for biomimetics study.
(3) For image-based 3-D modelling, especially for medical and animation applications, the techniques for edge detection and segmentation are more promising that point cloud based. This is due to the nature of data information and the methods for image data acquisition. But the accuracy could be a problem for many biomimetics studies.

#### 10.6.1.4. *3-D model creation*

Errors can be introduced in 3-D model creation. This is especially true for 3-D modelling of complex biological bodies with non-smooth features.[8,41]

### 10.6.2. *Limitations with data interpretation and sharing*

(1) Most software systems output the 3-D models in the formats that are very difficult for biomimetics researchers to understand. So even if some models are built, their potential cannot be fully exploited for biomimetics.
(2) Most software systems are Windows based, so 3-D models built by different people cannot be shared by others in an efficient way.

### 10.6.3. *Research interests in the areas of 3-D modelling of biological objects*

#### 10.6.3.1. *Analysis and synthesis of functions of biological systems*

It is critical to understand the underlying mechanics of biological systems for biomimetics research. Functional analysis and synthesis should be the first step for biomimetics research and applications. Simply copying geometrical features is not really what biomimetics research means. There are functional, structural, biologically evolutional reasons why biological systems exist in their existing shapes. The relationships between shapes and functions have to be established. Considerable work has been done. In particular, biologists have been making valuable efforts in areas such as functional, engineering and constructional morphology.[112,113] However, the interests of biologists are more in the explanation of why biological systems have those functions rather than from an engineering perspective. Besides, in nature most parts of organisms do two or more jobs. Usually our technology is interested in only a single function. So it is not scientifically meaningful and economically effective to simply learn the research results of biologists' work and copy biological systems for innovative product introduction. It is important to analyze and synthesize functions of biological systems from the biomimetics point of view based upon the biologists' work. This work should address issues such as:

(1) What functions of biological systems are economically meaningful for biomimetics study?

(2) Among all body shapes, what geometrical features are critical for those biological functions?
(3) The relationships between functions and shape geometry.
(4) Besides geometrical factors, are there any other important factors to support and dictate those functions? These factors can be chemical, physical and material properties, etc.
(5) All findings should be stored in data formats that are accessible to most computer systems (platform and computer software). The information should be easily interpreted by both biologists and engineers in order to do further analysis, simulation and even animation.

This work demands close collaboration between biologists, engineers, mathematicians, their colleagues in the fields of computing, chemistry and physics, as well as other related professions, coordinated by people who have expert knowledge and experience in biomimetics. Some valuable efforts have been made.[114]

The work in this area should lead to the requirements of 3-D modelling of biological systems. Documents should be organized to answer questions like what kinds of 3-D model are required and in which way the geometrical information is recorded and stored.

#### 10.6.3.2. *Methodology for 3-D modelling of biological objects*

Based on the requirements of 3-D biological objects in Section 10.3.1, the available 3-D scanning technologies/scanners, raw data processing algorithms, 3-D geometry computation theory and computer graphical visualization methods, work should be carried out to investigate all computer-based enabling 3-D modelling technologies to propose methodologies that can be used as a guideline (not a bible) for biomimetics researchers. However due to the fact that most existing 3-D modelling technologies have been developed for industrial, medical and animation purposes, one is very likely to reach the conclusion that it is impractical, if not impossible, to implement the proposed methodologies using just the existing technologies available on the market, which would demand new research and development work

leading to other research interests areas that will be addressed in the following sections.

The results of methodology proposition work should lead not only to some diagrams to depict the procedures for each methodology and documents to explain what should be done and how to do them, but also to the requirement documents for each technology used in various steps, their availability on the market, and study and development of new technologies.

#### 10.6.3.3. *New 3-D scanning system (scanners and associated software)*

From biologists' functional analysis of biological systems, we know some functions can be used as a clue/hint to or a "natural prototype" of an innovative product introduction. Then we begin to analyze this special function again from an engineering point of view. We often look around for a method of capturing geometrical information of the biological system. 3-D scanners are very likely our choice.

At the moment, it is technologically possible and economically viable to configure and build a 3-D scanner or purchase it from the commercial market. As seen in the discussion in Section 10.3, there are many 3-D scanners and associated software on the market. But they have been mainly built for industrial, medical and animation purposes. Therefore, they are suitable only for some biomimetics research. The functional limitations of existing 3-D scanners often lead to difficult situations for biomimetics research and applications.

As discussed in Section 10.6.1.1, the problems are typically either: (1) the workable area is big enough for a single setting/scanning but accuracy and resolution is low (most scanners industrial and animation and some scanners for medical applications) or (2) accuracy and resolution are high, but workable areas are too small (a few industrial scanners, some medical ones and most nano-technology ones). As far as the authors are aware, there are very few 3-D scanners available on the market that have been designed and developed specially for biomimetics research purposes. So we believe that it is necessary to design and develop 3-D scanning systems suitable for biomimetics research. The functional performance should be:

(1) The scanner's accuracy is probably as high as 0.5 $\mu$m to 1 $\mu$m.
(2) Ideally, scanners can capture both geometrical and color information with options choices for users.
(3) The scanning resolution is probably as high as 0.2 $\mu$m to 1 $\mu$m with adjustable ranges.
(4) The effective measurement ranges in x-, y- and z-directions should be large enough to capture most typical features of biological systems. It is arguable that the effective measurable areas in the x-y plane should not be less than 50 mm $\times$ 50 mm.
(5) The scanning force contact scanners can be pre-adjusted to low level to avoid deformation of body during scanning.
(6) The data can be exported to the other software systems either in their native formats or neutral formats such as IGES and STEP, etc.
(7) The technology used in the new systems should be reliable; special consideration should be given to various light source units (bulbs, for example) and mechanical adjustment mechanisms.

#### 10.6.3.4. *3-D computation theory and 3-D modelling software*

In the same way, most existing computation theory and mathematical models for 3-D modelling are suitable for industrial, medical and animation applications. They often require only point clouds and their polygonization for medical and animation applications. Bezier patches and NURBS mathematical models are suitable for a considerable portion of 3-D modelling of biological systems. But, as far as the authors are aware, there is little report of suitability studies to answer the question of which spatial geometry computation methods are suitable for 3-D modelling of which kinds of biological surfaces. Study in this area should cover:

(1) Geometrical feature analysis of typical biological surfaces to classify them into various primitive geometry features; the primitive features can be either as simple as those used in industry or a combination of them, or defined by using mathematical models such Bezier curves and NURBS.
(2) Performance analysis of typical mathematical models such as Bezier and NURBS for 3-D modelling of biological systems with

particularly features. For example, sharp tip corner of tarsus of insects.

(3) New methods for raw data pre-processing including noise filtering, point cloud sampling, and segmentation. These new methods should address the problems discussed in Section 10.5.1.

(4) Web-based mathematical modelling and presentation techniques.

(5) Theoretical study of a feature-based methodology for 3-D modelling of biological systems.

(6) Software should be designed and developed for 3-D modelling of biological systems. Besides the normal functions of most typical 3-D modelling software, some special modules should be included: (a) a data base that is accessible to the biomimetics community to store the pre-built class library (multi-media database) of modules of 3-D models of those primitive features defined in 1), (b) an animation module, (c) a module for outputting the explicit form of single curve and mathematical model based upon the user's instruction, and (d) a module for publication of geometrical information generated onto an information sharing portal over the World Wide Web.

(7) Software implementation should be with characteristics of platform independence, neutral file formats and ideally industrial standard (like XML) for information sharing.

## 10.7. Conclusion

To learn from nature, one of the fundamental issues is to understand the natural systems such as animals, insects, plants and human beings, etc. The geometrical characterization and representation of natural systems is an important fundamental work for biomimetics research. 3-D modelling plays a key role in geometrical characterization and representation, especially in computer graphical visualization. This chapter has presented the typical procedure of 3-D modelling methods and then reviewed the previous work of 3-D geometrical modelling techniques and systems developed for industrial, medical and animation applications. In particular, the chapter has discussed the problems associated with existing techniques and systems when they are applied

to 3-D modelling of biological systems. Three case studies have been presented to illustrate the applications of 3-D modelling to biomimetics research. Based upon the discussions, the chapter has proposed some areas of future research interest in 3-D modelling of biological systems and for biomimetics.

## References


[1] Vincent JFV. (2001) Stealing Ideas from Nature. In: Pellegrino S (ed.), *Deployable Structures*. Springer, Vienna, pp. 51–58.

[2] Vincent JFV, Bogatyreva OA, Bogatyrev NR, *et al*. (2006) Biomimetics: Its practice and theory. *Interface* **3:** 471–482.

[3] Zhang S, Hapeshi K, Ashok K, Bhattacharya AK. (2004) 3D Modelling of Biological Systems for Biomimetics. *Journal of Bionics Engineering* **1:** 20–40.

[4] Tong J, Guo ZJ, Ren LQ, Chen BC. (2003) Curvature features of three soil-burrowing animal claws and their potential applications in soil-engaging components. *International Agricultural Engineering Journal* **12:** 119–130.

[5] Ren LQ, Zhang L, Tong J, Shi YW. (2001) GA-based analysis of the fractalness of soil-burrowing animal body surfaces. *International Agricultural Engineering Journal* **10:** 13–27.

[6] Kobayashi H, Kresling B, Vincent JFV. (1998) The geometry of unfolding tree leaves. *Proc R Soc Land* **5:** 147–154.

[7] Tong J, Sun JY, Chen DH, Zhang SJ. (2005) Geometrical features and wettability of dung beetles and potential biomimetic engineering applications in tillage implements. *Soil and Tillage Research* **80:** 1–12.

[8] Li SW, Tong J, Zhang SJ, Chen BC. (2004) Geometrical modelling of the exterior configuration of a cattle hoof by reverse engineering technique. *Transactions of the Chinese Society of Agricultural Engineering* **20:** 156–160.

[9] Haas F. (1994) Geometry and mechanics of hind-wing folding in Dermaptera and Colroptera.M Phil thesis, University of Exeter, UK.

[10] Herbig A, Kull U. (1991) Leaves and ramification. *Proc 2nd Int Symp*. SFB 230 Part 2, Stuttgart, Germany, pp. l09–117.

[11] Kresling B. (1991) Folded structures in natural lesson in design. *Proc 2nd Int Symp*. SFB 230 Part 2, Stuttgart, Germany, pp. 155–161.

[12] Kesel AB. (1994) The insect wing — a multifunctional mechanical system. *Proc 3rd Int Symp*. SFB 230, Stuttgart, Germany, pp. 181–184.

[13] Wootton RJ. (1981) Support and deformability in insect wings. *J Zoot Land* **193:** 447–468.

[14] Okabe M. (2003) 3D modelling of trees from freehand sketch. BSc Thesis, University of Tokyo, Japan.

[15] Deussen O, Lintermann B. (1999) Interactive modelling of plants. *IEEE Computer Graphics and Applications* **19:** 56–65.
[16] Mech R, Prusinkiewicz P. (1996) Visual models of plants interacting with their environment. *Proceedings of SIGGRAPH* **96:** 397–410.
[17] Ghanem TA, Rabbitt RD, Tresco PA. (1998) Three-dimensional reconstruction of the membranous vestibular labyrinth in the toadfish. *Opsanus tau*. *Hearing Research* **124:** 27–43.
[18] Angelo J, Beraldin JA, Blais F, *et al.* (2000) Real world modelling through high resolution digital 3D imaging of objects and structures. *ISPRS Journal of Photogrammetry and Remote Sensing* **55:** 230–250.
[19] Gledhill D, Tian GY, Taylor D, Clarke D. (2003) Panoramic imaging — a review. *Computers and Graphics* **27:** 435–445.
[20] Huang D, Yan H. (2003) NURBS curve controlled modelling for facial animation. *Computers and Graphics* **27:** 373–385.
[21] Craig G, Cramer KE, Cody DD, *et al.* (1999) Premature partial closure and other deformities of the growth plate: MR Imaging and Three-dimensional Modeling. *Radiology* **210:** 835–843.
[22] Kim JS, Park TS, Park SB, *et al.* (2000) Measurement of femoral neck anteversion in 3D, Part 1: 3D imaging method. *Medical and Biological Engineering and Computing* **38:** 603–609.
[23] Kim JS, Park TS, Park SB, *et al.* (2000) Measurement of femoral neck anteversion in 3D, Part 2: 3D modelling method. *Medical and Biological Engineering and Computing* **38:** 610–616.
[24] Gruen A, Murai SJ. (2002) High-resolution 3D modelling and visualization of mount Everest. *ISPRS Journal of Photogrammetry and Remote Sensing* **57:** 102–113.
[25] Swingen CM, Seethamraju RT, Jerosch-Herold M. (2003) Feed-back-assisted three-dimensional reconstruction of the left ventricle with MRI. *Journal of Magnetic Resonance Imaging* **17:** 528–537.
[26] Pollefeys M, Koch R, Vergauwen M, Van Gool L. (2000) Automated reconstruction of 3D scenes from sequences of image. *ISPRS Journal of Photogrammetry and Remote Sensing* **55:** 251–267.
[27] Sarti A, Gori R, Lamberti C. (1999) A physically based model to simulate maxillo-facial surgery from 3D CT images. *Future Generation Computer Systems* **15:** 217–221.
[28] Han M, Kanade T. (2002) A perspective factorization method for Euclidean reconstruction with uncalibrated cameras. *The Journal of Visualization and Computer Animation* **13:** 211–223.
[29] Streicher J, Miiller GB. (2001) 3D modelling of gene expression patterns. *TRENDS in Biotechnology* **19:** 145–148.
[30] Behr J, Choi SM, Grokopf S, *et al.* (2000) 3D modelling for diagnosis and treatment planning in cardiology. *Radiologe* **40:** 256–261.

[31] Kehl HG, Jager J, Papazis N, *et al.* (2000) 3D heart modelling from biplane, rotational angiocardiographic X-ray sequences. *Computers and Graphic* 24: 731–739.

[32] Courrioux, G, Nullans, S, Guillen, A, *et al.* (2001) 3D volumetric modelling of Cadomian terrains (Nonhem Brittany, France): an automatic method using Voronoi diagrams. *Tectonophysics* **333:** 181–196.

[33] Zhang X, Zhang S, Hapeshi K. (2014) A New Parameterised Feature-based Generic 3D Human Face Model for Emotional Bio-robots. *Appl Mech Mater* **461:** 838–847.

[34] Sun J, Tong J, Chen D, Zhang S. (2014) Quasi-static and dynamic nanoindentation of some selected biomaterials. Journal of Bionics Engineering **11:** 114–150.

[35] Li M, Chen D, Zhang S, Tong J. (2014) Biomimetic Design of a Stubble-Cutting Disc Using Finite Element Analysis. *Journal of Bionics Engineering* **10:** 118–127.

[36] Zhang X, Zhang S, Hapeshi K. (2010) A New Method for Face Detection in Colour Images for Emotional Bio-robots. *Science China, Technological Science* **53:** 2983–2988

[37] Zang H, Zhang S, Hapeshi K. (2010) A Review of Nature-Inspired Algorithms. *Journal of Bionics Engineering* 7**S:** s232–s237.

[38] Wen H, Zhang S, Hapeshi K, Wang X. (2008) A Methodology for Innovative Product Design: Inspiration from Nature. *Journal of Bionic Engineering* **5:** 75–84.

[39] Zhang S, Tong J, Hapeshi K, *et al.* (2007) Optimising Body Layout Design of Limbed Machines — Observation from Nature and Theoretical Investigation, *Journal of Bionic Engineering* **4:** 117–122.

[40] Tamas V, Ralph RM, Jordan C. (1997) Reverse engineering of geometric models an introduction. *Computer Aided Design* **29:** 225–268.

[41] Zhang S, Raja V, Lim W, *et al.* (2002) Error analysis of data acquisition of reverse engineering process using design of experiment. In: Cheng K, Webb O (eds.), *Advanced Manufacturing Technology XVI.* Professional Engineering Publishing Limited, pp. 145–150.

[42] Renishaw. http://www.renishaw.com/client/product/UKEnglish/PGP-890.shtml (Accessed on 11-06-2015.)

[43] Wicks and Wilson. http://www.wwl.co.uk/ (Accessed on 11-06-2015.)

[44] 3D Cafe. http://www.3dcafestore.com/3dmodels1.html (Accessed on 11-06-2015.)

[45] 3Dlenta. http://3dlenta.com/en/plants.html (Accessed on 11-06-2015.)

[46] Anderson RC. (1982) Photograrnmetry: the pros and cons for archaeology. *World Archaeology* **14:** 200.

[47] Jeyapalan K. (1980) Photogrammetry in recording the historic ship iantic. *Photogrammetric Engineering and Remote Sensing* **46:** 15–31.

[48] Schenk I. (2005) Introduction to Photogrammetry. http://www.mat.uc.pt/~gil/downloads/IntroPhoto.pdf (Accessed 12-06-2015.)
[49] Urquhart CW, Sieben JP. (1993) Towards real-time dynamic close range photogrammetry. *Proc SPIE Videometrics II* **2067:** 240–251.
[50] Sieben JP, Marshall SJ. (2000) Human body 30 imaging by speckle texture projection photogrammetry. *Sensor Review* **20:** 218–226.
[51] William J, Wing N. Geometric Analysis, Visualization, and Conceptualization of 3D Image Data. Imaging and Distributed Computing Group, Information and Computing Sciences Division, Lawrence Berkeley Laboratory, Publication number: LBL-35329. http://froggy.lbl.gov/papers/Reports/LBL.35329.html (Accessed 05-06-2015.)
[52] Zhang S, Hapeshi H. (2014) 3D Geometry Modelling of Pores Copper Materials. Industrial Report, The University of Gloucestershire.
[53] Zhang S, Raja V, Ryall C, Wimpenny D. (2003) Rapid prototyping models and their quality evaluation using reverse engineering. *Journal of Mechanical Engineering Science* **217(C):** 81–96 .
[54] Jun YT, Raja VH. (2002) Extracting geometric attributes directly from scanned point set for feature recognition. *Int J of Computer Integrated Manufacturing* **15:** 50–61.
[55] Jun YT, Raja VH, Park S. (2001) Geometric feature recognition for reverse engineering using neural networks. *Int J of Advanced Manufacturing Technology* **17:** 462–470.
[56] Park S, Jun YT. (2001) Automated segmentation of scanned point data in feature-based reverse engineering system. 2001 I nternational CIRP Design Seminar. Stockholm, Sweden, pp. 353–358.
[57] Lindeberg T. (1998) Edge detection and ridge detection with automatic scale selection, *International Journal of Computer Vision* **30:** 117–154.
[58] Ziou D, Tabbone S. (1998) Edge detection techniques: An overview. *International Journal of Pattern Recognition and Image Analysis* **8:** 537–559.
[59] Canny J. (1986) A computational approach to edge detection. *IEEE Trans Pattern Analysis and Machine Intelligence* **8:** 679–714.
[60] Imageware Surfacer. http://www.dipro.co.jp/english/products/cad_cam/imageware/productfamily/index.html (Accessed 11-06-2015.)
[61] Raindrop Geomagic Studio. http://www.geomagic.com (Accessed 11-06-2015.)
[62] Faro 3D X330. http://www.faro.com/products/3d-surveying (Accessed 11-06-2015.)
[63] Mullins J. (1997) Secrets of a Perfect Skin: Sharks do it, dolphins do it — now even aircraft engineers are managing to banish turbulence and drag. *New Scientist* **2065:** 28.
[64] Ridgway SH, Carder DA. (1993) Features of dolphin skin with potential hydrodynamic importance. *IEEE Engineering in Medicine and Biology* **12:** 83–88.

[65] Zhang S, Howard D, Sanger D, Miao S. (1998) Multi-legged walking machine body designs. *Robotica* **16:** 593–598.
[66] Howard D, Zhang S, Sanger DJ. (1998) Multilegged walker design — the joint torque versus workspace compromise. *Journal of Mechanical Engineering Science* **212 (C):** 477–488.
[67] Chung A. (2002) Bionics information exchange portal system. MSc Thesis, University of Warwick, UK.
[68] Mitutoyo. http://www.mitutoyo.co.uk (Accessed 11-06-2015.)
[69] http://what-when-how.com/digital-imaging-for-cultural-heritage-preservation/processing-sampled-3d-data-reconstruction-and-visualization-technologies-digital-imaging-part-1 (Accessed 11-06-2015.)
[70] Reid GT, Rixon RC, Stewart H. (1998) Stripe scanning for engineering. *Sensor Review* **8(2):** 67–71.
[71] Reid GT, Marshall SJ, Rixon RC, Stewart H. (1988) A laser scanning camera for range data acquisition. *Phys D: Appl Phys* **21:** S1–S3.
[72] Reid GT, Rixon RC, Stewart H. (1988) Moire topography with large contour intervals. *Proc SPJE* **814:** 307–313.
[73] Isdale J. (1998) 3D scanner technology review. http://www.isdale.com/jerry/VR/3DScanners/3DScannerReview.html (Accessed 11-06-2015.)
[74] Stanford School of Medicine, 3D Reconstruction. http://biocomp.stanford.edu/3dreconstruction (Accessed 11-06-2015.)
[75] Stevens JK, Mills LR, Trogadis JE. (1994) *Three-dimensional Confocal Microscopy: Volume Investigation of Biological Systems.* Academic Press, London.
[76] MicroScribe. http://www.3d-microscribe.com/G2%20Page.htm (Accessed 11-06-2015.)
[77] Photogrammetry. http://www.realitymeasurements.com/crdp-low-altitude.htm (Accessed 11-06-2015.)
[78] Gerald EF. (1988) *Curves and Surfaces for Computer Aided Geometric Design: A Practical Guide*. Academic Press Inc, London.
[79] Gerald F. (1993) *Curves and Surfaces for CAGD (a Practical Guide)*, 3rd ed. Academic Press Inc, London.
[80] Josef H, Dieter L. (1993) *Fundamentals of Computer Aided Geometric Design*. A. K. Peters, Ltd, USA.
[81] Huang D, Yan H. (2003) NURBS curve controlled modelling for facial animation. *Computers and Graphics* **27:** 373–385.
[82] Piegl L, Tiller W. (1997) *The NURBS Book*, 2nd ed. Springer, Berlin.
[83] Wen H, Zhang S, Hapeshi H, Wang X. (2008) A Methodology for Innovative Product Design: Inspiration from Nature. *Journal of Bionic Engineering* **5:** 75–84.
[84] Cross N. (1984) *Developments in Design Methodology.* John Wiley, New York, USA.

[85] Edmonds E, Soufi B. (1992) The computational modelling of emergent shapes in design. In: Gero JS, Sudweeks F (eds.), *Computational Models of Creative Design*. University of Sydney, Australia.

[86] Raja V, Zhang SJ, Garside J, *et al.* (2006) Rapid and cost-effective design and manufacturing of high-integrity aerospace components. *International Journal of Advanced Manufacturing Technology* **27:** 759–773.

[87] Zhang X, Zhang S, Hapeshi K. (2014) A New Parameterised Feature-based Generic 3D Human Face Model for Emotional Bio-robots. *Applied Mechanics and Materials* **461:** 838–847.

[88] Hashimoto T, Hiramatsu S, Kobayashi H. (2006) Development of face robot foremotional communication between human and robot. *Proceedings of IEEE International Conferenceon Mechatronics and Automation (ICMA 2006)*, Luoyang, China, pp. 25–30.

[89] Takahashi Y, Hatakeyama M, Kanno M. (2007) Experiments on human facial expressions for improvement of simplified robot face. *Annual Conference SICE*, Takamatsu, Japan, pp. 480–483.

[90] Takahashi Y, Sato H. (2010) Compact robot face with simple mechanical components. *Proceedings of International Conference on Control Automation and Systems (ICCAS 2010)*, Gyeonggi-do, South Korea, pp. 2300–2303.

[91] Waters K, Terzopoulos D. (1991) Modelling and animating faces using scanned data. *The Journal of Visualization and Computer Animation* **2:** 123–128.

[92] Yongli H, Mingquan Z, Zhongke W. (2009) An automatic non-rigid point matching method for dense 3D face scans. *Proceedings of International Conference on Computational Science and Its Applications (ICCSA 2009)*, Suwon, Korea, pp. 215–221.

[93] Tognola G, Parazzini M, Svelto C, *et al.* (2003) A fast and reliable system for 3D surface acquisition and reconstruction. *Image and Vision Computing* **21:** pp. 295–305.

[94] Guenter B, Grimm C, Malvar H, Wood D. (1998) Making faces. *Proceedings of the 25thAnnual Conference on Computer Graphics and Interactive Techniques*, Orlando, FL, USA, pp. 55–66.

[95] Rydfalk M. (1978) *CANDIDE*, a parameterized face. PhD thesis, Linköping University, Linköping, Sweden.

[96] Ahlberg J. (2001) *CANDIDE-3* — an updated parameterised face. Report No. LiTH-ISY-R-2326, Dept. of Electrical Engineering, Linköping University, Sweden.

[97] Welsh B. (1991) Model-based coding of videophone images. *Electronics & Communication Engineering Journal* **3:** 29–36.

[98] Mayer C, Wimmer M, Stulp F, *et al.* (2008) A real time system for model-based interpretation of the dynamics of facial expressions. *Proceedings of 8th IEEE*

*International Conference on Automatic Face & Gesture Recognition (FG'08)*, Amsterdam, Netherlands, pp. 1–2.

[99] Blanz V, Vetter T. (1999) A morphable model for the synthesis of 3D faces. *Proceedings of the 26th Annual Conference on Computer Graphics and Interactive Techniques*, Los Angeles, USA, pp. 187–194.

[100] Davies A, Ek CH, Dalton C, Campbell N. (2012) Generating 3D morphable model parameters for facial tracking: factorising identity and expression, *Proceedings of the International Conference on Computer Graphics Theory and Applications and International Conference on Information Visualization Theory and Applications*, Rome, Italy, pp. 309–318.

[101] Au BL, Ly QN, Minh HP. (2012) An individualized system for face ageing and facial expressions modeling based on 3D practical faces data. *Proceedings of International Conference on Control, Automation and Information Sciences (ICCAIS)*, Saigon, Vietnam, pp. 398–403.

[102] Ahyoung S, Seong-Whan L, Bulthoff H, Wallraven C. (2012) A morphable 3D-model of Korean faces. *Proceedings of IEEE International Conference on Systems, Man, and Cybernetics (SMC)*, Seoul, Korea, pp. 2283–2288.

[103] He Y, Qin H. (2004) Surface reconstruction with triangular b-splines. *Proceedings of Geometric Modeling and Processing*, Beijing, China, pp. 279–287.

[104] Larrabee WF, Makielski KH, Henderson JL. (2004) *Surgical Anatomy of the Face*. Lippincott Williams & Wilkins, Philadelphia, USA.

[105] Rose EH. (1998) *Aesthetic Facial Restoration*. Lippincott-Raven, New York, USA.

[106] Sun N, Ayabe T, Nishizaki T. (2007) Efficient spline interpolation curve modeling. *Proceedings of the 3rd International Conference on Intelligent Information Hiding and Multimedia Signal Processing*, Splendor Kaohsiung, Taiwan, **2:** 59–62.

[107] Hartley PJ, Judd CJ. (1978) Parametrization of Bézier-type b-spline curves and surfaces. *Computer Aided Design* 10: 130–134.

[108] Boor CD. (1972) On Calculating with B-Splines. *Journal of Approximation Theory* **6:** 50–62.

[109] Zhang X, Zhang S, Hapeshi K. (2010) A new method for face detection in colour images for emotional bio-robots. *Science China Technological Sciences* **53:** 2983–2988.

[110] Meille S, Garboczi EJ. (2001) Linear elastic properties of 2D and 3D models of porous materials made from elongated objects. *Modelling Simul Mater Sci Eng* **9:** 371.

[111] Karageorgiou V, Kaplan D. (2005) Porosity of 3D biomaterial scaffolds and osteogenesis. *Biomaterials* **26:** 5474–5491.

[112] Gudo M, Gutmann M, Scholz J. (2002). Concepts of functional, engineering and constructional morphology: introductory remarks. Senckenbergiana lethaea **82:** 7–10.

[113] Schmidt K, Vogel KPJ. (1991) *Constructional Morphology and Evolution*. Springer, Berlin, Heidelberg, New York, Tokyo.
[114] Vincent JFV, Mann DL. (2002) Systematic technology transfer from biology to engineering. *Phil Trans R Soc A* **360:** 159–174.